N and C-14 Content of Spent Fuel

P. Marimbeau[1], E. Esbelin[2]

[1]CEA/DEN/Cadarache, DER/SPRC, pmarimbeau@cea.fr
[2]CEA/DEN/Marcoule, DRCP/SE2A, eric.esbelin@cea.fr

Introduction

The PRECCI Program (*Programme de Recherche sur l'Evolution à long-terme des Colis de Combustibles Irradiés* – Long-term Evolution of Spent Fuel Packages Research Program) brings together all the CEA projects on the long-term behavior of spent fuels. PRECCI is supported by several French industrial partners: EDF, FRAMATOME-ANP, COGEMA and ANDRA.

PRECCI [1,2] is a R&D program intended to obtain the technical and operational data required to describe the behavior, under safe conditions, of spent fuel in long-term storage or disposal. The program should quickly provide relevant technical indicators that can be used to characterize spent fuel packages, predict their long-term behavior in the context of storage or disposal and possibly modify the storage concepts to the requirements imposed by the spent fuel packages.

Studies are divided into several sub-programs, each of which covers a specific theme. Sub-program 1 (SP1), for example, is dedicated to producing intrinsic Reference Data for spent fuel and the **source term** for the other PRECCI sub-programs. On this subject it is essential that calculated physical quantities (inventory, activities, etc.), particularly estimates for isotopes of interest to PRECCI, should be **qualified** and include a justified uncertainty. This requires that a database of experimental analytical results was previously available, possibly broadened to include new isotopes if necessary.

Choosing which isotopes are of interest is done on the basis of studies such as work to prioritize radio-nuclides performed by a special Working Group. We have to make distinctions between various categories of package, spent fuel, glass derived from reprocessing and hulls. By taking several different time-scales ranging up to one million years in the future, and making conservative assumptions on the deterioration of packages and the chemical mobility of elements, a certain number of isotopes stand out as significant at particular points in time. These main isotopes include obviously the actinides and some long-lived fission products, but also activation products, some of which are produced due to the activation of impurities.

Calculating the source term using DARWIN – CESAR:

Presentation of the Package

DARWIN (Development Applied to Recycling, Verified and Validated for Nuclear facilities – Installations in French) is the French Reference Package for the fuel cycle [3,4]. It is devoted to provide the required parameters concerning the fuel cycle (figure 1) and is based on the JEF2.2 evaluation of basic nuclear data [5]. Neutronic calculations are performed by APOLLO-2 – the reference code system for neutronics in water reactors – using the CEA93 multigroup library which is also elaborated from JEF2.2. It produces cross-sections and neutron spectrums characteristic of objects (rods, assemblies, etc.) that have evolved during their lifetime in the reactor. The PEPIN-2 evolution module is next provided with these neutronic data and with libraries of cross-sections and nuclear constant - in order to fill in, depending on the filiation chains selected, the sections and/or isotopes of APOLLO-2. Thus JEF2.2 will be completed by using EAF99 estimation for activation products.

During evolution according to the history provided, the PEPIN-2 code calculates the concentrations; a post-treatment module is used next to access the various physical quantities deduced: inventories, activities, residual power, neutron emission, n and γ emission spectrums, toxicities, etc. It should be noted that the filiation chains in DARWIN are complete, i.e. they include all the isotopes and therefore all the filiations for which basic nuclear data are present.

The neutronic calculation scheme used in DARWIN uses again the optimized calculation modelling developed in order to qualify the neutronic system. In particular, the treatment of MOx fuel assemblies irradiated in a composite core at 30 % MOx requires that the surrounding UO_2 assemblies be accounted for [6,7].

The calculation scheme with PEPIN-2 has a variant with the CESAR evolution code which was developed for industrial use in cooperation with COGEMA. The constitution module of the BBLs compiled for CESAR is provided with the same cross-sections and spectrums supplied by APOLLO-2 as PEPIN-2, with the difference that cross-sections are first fitted depending on the burnup. Depletion calculations in CESAR are faster than those of PEPIN-2 and relate to a limited number of isotopes – in fact, those which are useful – with fixed filiation chains. The physical parameters available at the end of processing are the same. Once the coherence of the basic data and the filiation chains has been checked, and after comparison of the results from the two codes, qualification of DARWIN may be transposed directly to CESAR.

CESAR is the code used to constitute the PRECCI Reference Base of Intrinsic Data for spent fuel on a set of representative UOx and MOx managements.

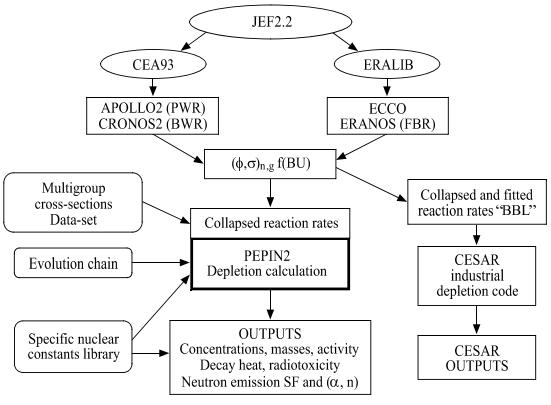

Fig. 1: The DARWIN-CESAR package

Qualification of the DARWIN package

Qualification of DARWIN is based on a wide range of isotopic analyses performed on pieces of spent fuel rods from electricity-generating reactors – mainly 17x17 PWRs. These analyses are carried out in collaboration with our French industrial partners EDF and FRAMATOME-ANP and mainly use mass spectrometry.

Qualification domain covers [8] :

- UOx fuels up to burnup of 60 GWd/t;

actinides analyzed: Uranium, 234 to 238,
Plutonium, 238 to 242,
Neptunium 237,
Americium, 241 to 243,
Curium, 243 to 247.

FPs analyzed: Cesium, 133 to 137,
Neodymium, 143 to 150,
Credit Burn Up FPs ^{149}Sm, ^{103}Rh, ^{143}Nd, ^{133}Cs, ^{155}Gd, ^{151}Sm, ^{152}Sm, ^{99}Tc, ^{145}Nd, ^{153}Eu, ^{95}Mo, ^{147}Sm, ^{150}Sm, ^{109}Ag and ^{101}Ru.

Metallic FPs can generate certain insoluble components and therefore require complete dissolution with re-working of dissolution fines : this treatment is in process.

- MOx fuels up to burnup of 45 GWd/t. The same isotopes are analyzed and the condition is the same for Credit Burn Up FPs.

Figure 2 shows Calculation-Experimental discrepancies for UOx and MOx fuels.

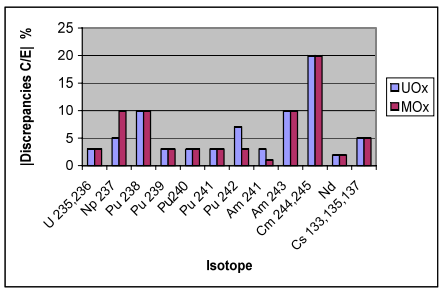

Fig. 2: State of qualification of DARWIN-CESAR

The need for a specific analytical program

The realization that there was no qualification for certain important isotopes in PRECCI – particularly all the impurities activation products (IAP) – led to the creation of a specific analytical program; the established analytical programs on high burnup fuels such as HTC and MALIBU continued simultaneously.

In addition, the importance according to certain IAPs, justified research to establish better data on initial impurity content. This led to the launch of a statistical study on fabrication analyses – oxide fuels and structural materials. It should be noted that in order to interpret measurements of the abundance of some IAPs, the initial content in the source element needs to be known with sufficient accuracy.

The PRECCI analysis program is designed to measure the abundance of 3 groups of long-lived radionuclides in UOx and MOx fuels at two burnup, a high value and an intermediate value (60 and 35 GWd/t):

- Long-lived fission products: ^{79}Se, ^{90}Sr, ^{93}Zr, ^{107}Pd and ^{126}Sn (^{135}Cs and ^{99}Tc are measured elsewhere);

- Impurity activation products of oxide: ^{59}Ni, ^{93}Mo and ^{94}Nb;
- Gaseous or volatile products: ^{14}C, ^{36}Cl and ^{129}I.

After a phase in which the measuring techniques were debugged, the first results are now being obtained. The only exception is ^{36}Cl which is still in the R & D phase.

Formation of Carbon 14

^{14}C is a crucial isotope in terms of waste management; its 5,730-year half-life means that it still has a major impact after more than 10,000 years and it has a special chemical affinity with the environment.

Channels of formation

^{14}C is an activation product essentially formed by oxygen and nitrogen activations ; it is also FP of ternary fission. The capture cross-sections of carbon natural isotopes, ^{12}C and ^{13}C, are very low (of the order of mb), which means that ^{14}C production from carbon remains negligible except for carbide or HTR type fuels.

The main channels of formation are as follows:

- ^{14}N (n,p) ^{14}C ; ^{14}N accounts for virtually all the nitrogen (99.63 %)
- ^{17}O (n,α) ^{14}C ; ^{17}O accounts for 4 10^{-4} of the Oxygen
- ^{16}O (n, ^{3}He) ^{14}C ; ^{16}O accounts for virtually all the Oxygen (99.76 %)
- ^{18}O (n, nα) ^{14}C ; ^{18}O accounts for 0.20 % of the Oxygen
- ternary fissions with fission yields of the order of 10^{-6}.

The first two cross-sections, which are responsible for main filiations, range across the entire energy spectrum and yield the highest reaction rates (Figure 3). The other two are threshold reactions that are limited to high-energy neutrons.

Table 1 shows contributions for oxide fuels (UOx and MOx) at 50 GWd/t to the formation of ^{14}C. Main contribution is that from oxygen; but oxygen is an important constituent in fuel oxide, while nitrogen is only an impurity (< 10 ppm).

In oxygen-free fuels or structural materials, the nitrogen impurity is the main source of ^{14}C.

Tab. 1: Formation of ^{14}C for fuels at 50 GWd/t

Filiations	Contribution (%)	
	UOx	MOx
^{17}O (n, α) ^{14}C	59.6	63.5
^{14}N (n, p) ^{14}C	35.6	27.9
ternary fission → ^{14}C	4.1	7.8
^{16}O (n, ^{3}He) ^{14}C	0.23	0.35
^{16}O (n, α) ^{17}O (n, α) ^{14}C	0.22	0.19
^{18}O (n, nα) ^{14}C	0.14	0.20

Given the channels of formation, the abundance of ^{14}C formed is approximately proportional to the burnup (or to the fluence). In the case of MOx fuel, formation by fission is slightly higher because the fission yield is higher for Pu than for ^{235}U; but in this hardened MOx spectrum, the entire formation is reduced by approximately 10 %.

Estimated abundance of ^{14}C

In a type AFA-2G 900 MWe - PWR 17x17 assembly (FRAMATOME-ANP), the material masses are as follows:

- 521 kg of UO_2 or 460 kg of heavy metal (Uranium) for a UOx assembly,
- 514 kg of oxide or 453 kg of heavy metal for a MOx assembly,
- 125.6 kg of zircaloy 4,
- 2.14 kg of Inconel 718,
- and 16.37 kg of steel 304.

Table 2 shows the calculated masses of ^{14}C present in a 900 MWe assembly (in grams); calculations are for a range of cooling times ranging from 10 to 10,000 years.

Tab. 2: Masses of ^{14}C in grams contained in an AFA-2G 900 MWe assembly

Masses of ^{14}C in the assembly for cooling time of	10 years	300 years	3,000 years	10,000 years
Fuel UOx – 33 GWd/t	4.09^{E}-2	3.95^{E}-2	2.85^{E}-2	1.222^{E}-2
Fuel MOX – 37 GWd/t	3.67^{E}-2	3.54^{E}-2	2.55^{E}-2	1.095^{E}-2
Fuel UOx – 50 GWd/t	5.72^{E}-2	5.52^{E}-2	3.98^{E}-2	1.707^{E}-2
UOx assembly structures at 50 GWday/t	**10 years**	**300 years**	**3,000 years**	**10,000 years**
Zircaloy4	2.51^{E}-2	2.42^{E}-2	1.747^{E}-2	7.49^{E}-3
Inconel 718	3.15^{E}-4	3.05^{E}-4	2.20^{E}-4	9.42^{E}-5
Steel 304	1.28^{E}-2	1.23^{E}-2	8.91^{E}-3	3.82^{E}-3

The evolved compositions of the structures are determined using a calculation in which the assembly is represented as being divided into 7 axial zones, in order to give the best reproduction of the distribution of the flux and of the spectrum. The contribution in ^{14}C from the structures accounts for approximately 2/3 of that from the fuel.

Work on impurity contents

In the recent past the IAPs were calculated on the basis of the initial content given in the manufacturers' specifications. This approach certainly yielded values on the high side; but if this type of overstatement is uncontrolled it can prove too conservative.

For the purposes of PRECCI it was therefore decided to launch a statistical study of the manufacturers' analyses of batches of industrially produced components. The study looked at significant masses and produced representative values for all manufactured items. This work was carried out in collaboration with the project's industrial partners: EDF, FRAMATOME-ANP and COGEMA and enabled us to compile a set of recommended values for the main materials. (These values cannot yet be made available other than to the partners in PRECCI).

For fuel oxides the results of the compilation are often flawed by the limit of detection imposed by the measuring technique used – **limit of detection for nitrogen of 8 ppm in UOx and MOx fuels**. – Despite this limitation the gain over the initial specifications is often of the order of a factor of 10.

In Table 3, by using these recommendations the estimated activities of several IAPs are given by "gram of initial heavy metal" for a UOx fuel irradiated at 50 GWd/t_{HM}.

Tab. 3: Activities of some important IAPs in Bq/g_{HM} for 50 GWd/t UOx fuel

Activities in UOx fuel for cooling time of	10 years	300 years	10,000 years
^{3}H (FP and IAP)	1.500^{E}+7	1.246	0.0
^{14}C (IAP and FP)	2.05^{E}+4	1.978^{E}+4	6.12^{E}+3
^{36}Cl	5.37^{E}+2	5.37^{E}+2	5.25^{E}+2
^{41}Ca	7.60^{E}+1	7.59^{E}+1	7.11^{E}+1
^{59}Ni	1.387^{E}+2	1.383^{E}+2	1.265^{E}+2
^{63}Ni	1.984^{E}+4	2.66^{E}+3	0.0
^{93}Mo	2.28^{E}+2	2.15^{E}+2	3.15^{E}+1

The international benchmark on evolution codes

The experimental results are interpreted using DARWIN as they are obtained. Once the uncertainty has been included, discrepancies between calculated and experimental results are analyzed and cross-checked. The tendencies they reveal are transmitted to evaluations of the basic data.

One of the main objectives of PRECCI is to obtain the best-qualified basis possible for the characterization of spent fuels. The PRECCI project therefore decided to launch an international benchmark on evolution codes applied to fuel cycle. The initiative was accepted by the "Working Party on Plutonium Recycling" (WPPR) of the OECD and several teams declared their interest in it.

This exercise relates firstly to inventories since it is from inventories that the other physical parameters are deducted. It also aims to let each participant use its own tools to provide results : its codes, its calculation schemes, its basic nuclear data, etc. This benchmark focuses on the fuel cycle and the back-end of cycle, and in the initial phase at least on PWR fuels – UOx and MOx. The specifications are currently being drafted.

Measurement of ^{14}C in PRECCI

Developing the ^{14}C measuring process is the responsibility of ATALANTE team of E. ESBELIN at Marcoule.

Given that carbon is found in fuel in several chemical forms, that the abundance of ^{14}C is very slight and that a quantitative measurement requires that every trace be included, the main technical difficulties that need to be solved are as follows:

- Oxidizing all the carbon present in the fuel,
- Trapping all the CO_2 formed,
- Ensuring efficient enough purification to measure the ^{14}C using liquid scintillation with a satisfactory degree of accuracy.

In fact, as there is no direct method for measuring ^{14}C on dissolution – using Secondary Ion Mass Spectrometry (SIMS) on a pellet would be too tricky for quantitative measurements – and

as we have no reference value in the spent fuel, we need to proceed using comparative tests on the process of oxidation and desorption of ^{14}C. In the absence of any reference, it will also be accepted that if two processes are independent and yield the same maximum, reproducible values, then this result is quantitatively acceptable.

The selective trapping of ^{14}C is aimed at eliminating isotopes that cause interference during β analysis, in particular ^{129}I, ^{134}Cs, ^{137}Cs and ^{106}Ru. It is validated by X and γ spectrometry on the purified sample.

After several tests, our chosen methods are considered to have been validated. We obtain accuracy of the order of $\pm$ 10 %. These first results are coherent as a first approximation with the CESAR estimations.

The results on the first sample of the PRECCI program are currently being obtained ; a full interpretation will enable us to evaluate the quality of the calculated estimate of ^{14}C.

References

C. POINSSOT et al., "Synthesis on the Long-term Behavior of the Spent Nuclear Fuel", Rapport CEA -R 5958 (2001).

C. POINSSOT, P. TOULHOAT, J.M. GRAS, P. VITORGE, "Long term Evolution of spent fuel in long term Storage and geological Disposal. Status of the French research program PRECCI", Actinides 2001, Japan (2001).

P. MARIMBEAU et al., "The DARWIN Fuel Cycle Package. Procedures for Material Balance Calculation and Qualification", ENC'98, Nice, France, October 25-28 1998.

A. TSILANIZARA et al., "DARWIN: an Evolution Code System for a large Range of Applications", ICRS-9, Tsukuba, Japan, October 1999.

JEFF Report 17, "The JEF2.2 Nuclear Data Library", May 2000.

C. CHABERT, A. SANTAMARINA, P. BIOUX, "Elaboration and experimental Validation of the APOLLO2 depletion transport route for PWR Pu Recycling", PHYSOR 2000, Pittsburg, USA, 2000.

C. CHABERT, A. SANTAMARINA, P. BIOUX, "Trends in nuclear data derived from integral experiments in thermal and epithermal reactors", Proc. Int. Conf. on Nuclear Data, Tsukuba, Japan, September 2001.

B. ROQUE et al., "Experimental Validation of the code system DARWIN for spent fuel isotopic predictions in Fuel Cycle Applications", Proc. Int. Conf. PHYSOR 2002, Seoul, Korea, October 7-10 2002.

^{14}C in a graphite reflector – method development and measurement of organic and inorganic ^{14}C

Å. Magnusson, K. Stenström, M. Faarinen, R. Hellborg, P. Persson and G. Skog
Department of Nuclear Physics, Lund University, Box 118, SE-221 00 Lund, Sweden
asa.magnusson@nuclear.lu.se

Abstract

The organic and inorganic ^{14}C fractions were measured in ten samples from a graphite reflector, previously used in a Swedish research reactor. For this purpose, a combustion and CO_2 absorption system was constructed and optimized. The optimized system proved excellent performance regarding complete oxidation and CO_2 absorption. The mean values of organic and inorganic ^{14}C in the ten samples were 519 and 1033 Bq/g, respectively. The summation of errors arising during the combustion and measuring procedure gave a total error of 3 - 20 % of the obtained results.

Introduction

Classification of waste material from nuclear facilities requires that the content of different radionuclides is known. In the case of ^{14}C the fractions of organic and inorganic ^{14}C are of special interest. The difference between organic and inorganic carbon compounds (when dealing with disposal issues) is that the inorganic carbon is affected by retention mechanisms such as sorption and precipitation, whereas the organic content is not. The fraction of organic ^{14}C is therefore – because of its mobility – a crucial parameter when modelling and predicting future release and migration of air- as well as waterborne ^{14}C after disposal.

The aim of this project, commissioned by the Swedish Nuclear Fuel and Waste Management Co. (SKB), was to develop a suitable method for measuring the fractions of organic and inorganic ^{14}C in samples from a graphite reflector. The reflector was a part of the first Swedish research nuclear reactor that was in operation between 1955 and 1970. The reactor was heavy-water-moderated and cooled, and used natural uranium as fuel. The permitted power was increased over the years from 0.1 to 1 MW_t (Lundgren and Ingemansson, 2001). The reflector was 0.9 m thick and made of graphite boulders, with a total amount of 52 tonnes, and cooled with air. The reactor parts were dismantled in the beginning of the 80´s and now await classification before final disposal. When dismounting the reflector, the graphite boulders were cut into pieces and placed in 95 steel boxes for storage.

The majority of the ^{14}C present in the graphite reflector is produced by the $^{14}N(n,p)^{14}C$ reaction. The second contributor is the $^{13}C(n,\gamma)^{14}C$ reaction. The nitrogen in the graphite comes from impurities arising during the graphite manufacturing process – from trapped air or impurities within the virgin material – with additional contamination arising through adsorption of nitrogen from the air, used to cool the reflector. The ^{14}C atoms formed by the $^{14}N(n,p)^{14}C$ reaction have a complex distribution, depending on the initial location of the nitrogen impurities. Generally, the ^{14}C is present in the regions where the nitrogen was adsorbed onto the surface and pores and generally bound into the structure (Marsden *et al.* 2002). According to Takahashi *et al.* (1999), who examined various samples of reactor graphite, the nitrogen content

was largest on the graphite surface, with a sharp decrease with depth (30 nm level examined). Since the ^{13}C atoms are randomly distributed in the graphite structure, the ^{14}C atoms formed from reaction with ^{13}C will have the same distribution (Marsden *et al.* 2002).

Very little is known about the chemical form of ^{14}C within the graphite and only a few references in the literature can be found on this topic. According to Marsden *et al.* (2002), some ^{14}C atoms formed in the graphite may be chemically compounded with hydrogen, nitrogen or oxygen atoms. It is also known from experience in a Canadian CANDU plant (heavy-water-moderated) that irradiation of nitrogen annulus gas produced ^{14}C, which was chemically combined with nitrogen, oxygen and hydrogen, and that the originally formed ^{14}C atoms were rapidly converted into simple hydrocarbons or carbon-nitrogen compounds (Greening, 1989). The compounds were found as deposits on stainless-steel components of the pressure tubes. According to Marsden *et al.* (2002), ^{14}C in the form of metal carbides is unlikely to be found in the graphite, due to the high temperatures needed for the formation.

Previous measurements of total ^{14}C in moderator and reflector graphite have been conducted by *e.g.* Bisplinghoff *et al.* (1999), Bushuev *et al.* (1999) and Bushuev *et al.* (1992).

In the present study, graphite samples from ten different boxes have been analyzed. The total amount of material representing one sample has been estimated to 500-1700 mg. No data exists on how the boxes and corresponding samples are related to the location within the reflector. To perform the required measurements, a combustion and CO_2 absorption system has been constructed and optimized. The system separates two fractions, referred to as organic and inorganic, respectively. These are separated by means of their different thermal stabilities. The organic fraction is here defined as compounds oxidized below 600 °C and the inorganic as compounds (mainly carbonates) oxidized between 600 °C and 900 °C.

The ^{14}C activity in the absorbed CO_2 from each combusted sample has been measured by a liquid scintillation counter. Besides ^{14}C the graphite also contains ^{152}Eu and ^{154}Eu. Therefore, these nuclides must be excluded before reaching the absorption system not to cause interference during the liquid scintillation analysis.

In this paper the combustion and absorption system is outlined as well as the system performance. Some measurements are presented and the quality of these is discussed.

Material and Methods

Previous methods for analyzing the content of organic and inorganic ^{14}C in soil have been documented by Milton and Brown (1993). The technique for analyzing soil containing less than 10 % of organic matter has been used as a starting point for our development. In the referred method the sample is combusted in a flow of oxygen (0.3 l/min) in a tube furnace together with a cupric oxide catalyst and the generated CO_2 is absorbed in 4M NaOH. The temperatures set for the combustion of the organic and inorganic fractions are 600 °C and 900 °C, respectively. The absorption is followed by either precipitation as carbonate or directly released into a scintillation cocktail.

Bisplinghoff *et al.* (1999) have determined the total ^{14}C activity in graphite samples from a reflector using 800 °C and a flux of 0.002 l/min of oxygen. Using these parameters it took them two hours until one gram of graphite was burned away completely.

Thermal methods are frequently used for determination of organic carbon (OC) and elemental carbon (EC) in aerosols. These fractions are also separated by means of their different thermal

stabilities. The EC fraction is however not identical to graphite carbon, but resistant to oxidation below 400 °C. Reviewed methods in Schmid *et al.* (2001) to determine the OC and EC fractions in aerosols involve oxidation of OC at 340 °C in a flow of oxygen, and oxidation of EC at temperatures between 650 °C and 800 °C. According to Petzold *et al.* (1997), only 1 % of $CaCO_3$ is oxidized at 650 °C.

Combustion and CO_2 Absorption System

Our optimized system is schematically outlined in Figure 1. The system consists of two tube furnaces; one for combustion of the sample and the other one with a catalyst to assure complete oxidation. The catalyst is placed separately because of the presumed broad range of combustion temperatures for the different carbon compounds within the graphite samples. This means that the catalyst has to have a very broad working temperature if placed in the same furnace as the sample. By using a separate furnace for the catalyst, optimum working conditions can always be maintained. The catalyst used consists of platinum on alumina beads (3.2 mm pellets) mixed with copper oxide wire (0.65 mm × 3 mm). After the catalyst tube furnace an empty wash bottle surrounded by ice is located in order to condense any compounds with europium. This ice trap is followed by a two-way valve and four gas washing bottles, placed in two series for the absorption of CO_2 from the organic and inorganic fractions of ^{14}C. When adjusting the system parameters, care has been taken to assure complete absorption of CO_2 in the first wash bottle in each series. This means that the second wash bottle could be used to monitor the absorption process and to widening the safety margins.

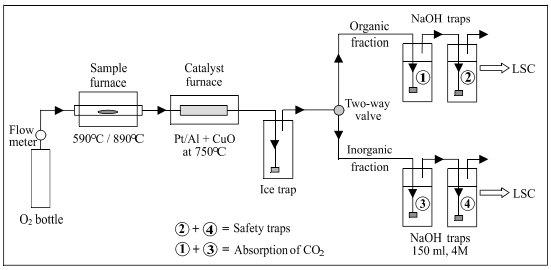

Fig. 1: Outline of the combustion and CO_2 absorption system

When operating the system, about 100 mg of sample material is placed in a combustion boat and inserted into the centre of the sample furnace. The four wash bottles are filled with 150 ml of 4M NaOH and the catalyst tube furnace is set to a temperature of 750 °C. A flowrate of oxygen of about 0.2 l/min is used to draw the combustion gases through the system. The organic fraction of ^{14}C is combusted at (590 ± 5) °C during 25 minutes (taking about 10 minutes to reach this temperature). Thereafter the two-way valve is switched to gas washing bottles 3 and 4

and the inorganic fraction is combusted at (890 ± 5) °C during 10 minutes (taking 7 minutes to reach this temperature).

Further information about the system can be found in *Magnusson* (2002).

Liquid Scintillation Analysis

The liquid scintillation counter used (LKB Wallac- Model 1217 Rackbeta) is equipped with an external standard used for determination of sample quench. The sample quench is determined from the External Standard Ratio (ESR), which according to a previously obtained quench curve corresponds to a certain efficiency. The quench curve was obtained using a set of 10 quenched standards (Packard Instrument Co.)

For liquid scintillation counting (LSC), two samples of each 2 ml were taken from the wash bottles and mixed with 18 ml of scintillation cocktail (Hionic-Fluor, Packard Instrument Co.) in glass vials. At the same time, two samples of each 2 ml were taken from the unused NaOH solution and mixed with scintillation cocktail as background samples. The vials were allowed to rest for at least 12 hours before counting. Each sample was then counted for 9000 s, giving a statistical error of 1.4-1.9 % (the latter referring to the background samples).

System Performance

Combustion and CO_2 Absorption System

To test whether the optimized system achieved complete oxidation, rest gases from the end of the system were collected during sample combustion and analyzed with a Fourier Transform InfraRed (FTIR) Spectrometer (see *e.g.* Hollas, 1996). The obtained spectra showed no signs of CO. Neither were there any visible signs of remaining sample material ever found in the combustion boat. This means that both combustion and oxidation of the samples could be considered as complete. The performance of the catalyst was also tested during the optimization procedure using two different types of carbon compounds: CO and CH_4. Both compounds were found to be completely oxidized.

To assure complete CO_2 absorption, the obtained FTIR spectra were also scanned for signs of CO_2, without finding any. LSC measurements of the samples collected after every sample combustion from wash bottle 2 and 4 (safety traps) showed no activity above the background level (with one exception). These facts strongly indicate that all CO_2 generated at the combustion was fully absorbed in the first wash bottles, *i.e.* 1 and 3, which means that no activity was lost to the surroundings.

To be sure that the method was reproducible and that no mistakes or mix-ups had been made during the combustion, material from two of the samples was combusted and measured twice (R1-108 and R1-093) and material from another sample three times (R1-058). A very good agreement was seen in the two measurements of sample R1-093 (see Table 1). When it comes to R1-058, the fraction of organic ^{14}C varies with 19 % between the highest and lowest obtained results and the fraction of inorganic ^{14}C with 11 %. The total sum of ^{14}C varies with 8 % at most. The total sum of ^{14}C for R1-108 varies with 5 %, the organic fraction with 18 % and the inorganic fraction with 12 %. Since each sample, taken from the graphite boulders, contained about 500 mg-1700 mg of material, the sub sample (100 mg) taken for analysis might not be representative for the whole sample if it is inhomogeneous regarding ^{14}C. The variations seen above are therefore probably due to the occurring variations of ^{14}C concentration within the bulk

sample. An additional cause of the variations is the errors arising during the combustion and the measuring procedure (see "Uncertainties" below).

Cross contamination has been avoided by carefully undertaken decontamination procedures after each sample combustion. The degree of decontamination was tested by performing blank sample combustions after ordinary graphite combustions. The results showed that there were no signs of activity above background level in either of the samples taken from the wash bottles.

The ^{14}C recovery of the system is estimated to be nearly 100 %. This was confirmed by combusting the most active sample (R1-058) a fourth time followed by a blank sample combustion, where the decontamination procedure was omitted. The resulting blank samples, taken from the wash bottles, did not show any signs of remaining ^{14}C. This, together with the fact that the CO_2 absorption is complete and that no signs of remaining sample material ever was seen, constitute the basis of the estimated ^{14}C recovery. However, obtained beta spectra from the blank samples showed a contamination, which was identified as ^{3}H. The contaminant was also present in the LSC samples obtained from the fourth combustion of R1-058, accounting for 40-50 % of the total activity. The contamination was not present in the system before the recovery test, *i.e.* the contamination appeared after the measurements of the graphite samples. The contaminant is therefore believed to come from the surrounding environment in the radioactive lab, since the system had been left open for about four weeks between the ordinary measurements and the recovery test.

Gamma-spectrometry of three different samples from gas washing bottle 1 and 3 did not show any signs of Eu, nor did the obtained sample spectra, which means that compounds containing Eu were believed to have condensed in the Eu-trap.

Liquid Scintillation Counting

Samples with known activity have been measured to verify the reliability of the LSC method and the quench curve used. A labelled ^{14}C standard (Packard Instrument Co.) and a urine sample were measured. The urine sample had earlier been measured with Accelerator Mass Spectrometry (AMS, see *e.g.* Stenström, 1995). The mean value, obtained from four separate LSC measurements of the urine sample, showed to be within the error limits of the AMS- and LSC-methods (AMS result = 7.6 ± 0.4 Bq/ml and LSC result = 7.55 ± 0.19 Bq/ml). The four results showed an internal difference of 7.7‰. The results did not show any signs of chemiluminescence or static electricity, which otherwise would have disturbed the analyze. The labelled unquenched ^{14}C standard was measured three times. The difference between the true and the obtained result was less than 1‰.

Results

The results from the measurement of the fractions of organic and inorganic ^{14}C in the ten samples taken from the graphite reflector are seen in Table 1. As can be seen from the table, results from gas washing bottle 2 and 4 are lacking, as no activity above background level was found (with one exception). The inorganic ^{14}C content is about twice as much as the organic ^{14}C. The activity in the two samples taken from the same gas washing bottle differs with ≤4.4 %, with a mean value of 1.6 %. Calculated from the mean values obtained from these ten samples, the total amounts of organic and inorganic ^{14}C in the 52 tonnes of graphite are 27 GBq and 54 GBq, respectively.

Tab. 1: Organic and inorganic ^{14}C fractions obtained from measurement of ten samples from the graphite reflector, including the reproducibility measurements, (background subtracted)

Two samples (2 x 2 ml) were taken from each of the gas washing bottles. The values presented are those that are at least 3 standard deviations above background level (except one of the samples from wash bottle 2, for R1-109, which showed 0.03 Bq/ml).

Sample	Weight g	Organic ^{14}C Bq/ml		Inorganic ^{14}C Bq/ml		Organic ^{14}C Bq/g (mean value)	Inorganic ^{14}C Bq/g (mean value)
		Gas washing bottle 1		Gas washing bottle 3			
R1-020	0.100	0.30	0.30	0.67	0.68	443	1011
R1-030	0.107	0.10	0.09	0.27	0.26	131	371
R1-045	0.118	0.28	0.27	0.87	0.86	346	1104
R1-055	0.095	0.46	0.48	0.86	0.87	596	1099
R1-058	0.100	1.13	1.12	1.71	1.72	1685	2573
R1-058	0.094	0.88	0.89	1.88	1.85	1370	2800
R1-058	0.110	1.16	1.17	2.12	2.14	1629	2907
R1-088	0.097	0.38	0.35	0.16	0.15	570	238
R1-093	0.111	0.06	0.06	0.28	0.28	77	376
R1-093	0.103	0.06	0.05	0.26	0.26	76	377
R1-108	0.106	0.22	0.18	0.74	0.71	278	1026
R1-108	0.105	0.23	0.23	0.58	0.62	337	901
R1-109	0.107	0.52	0.48	1.31	1.34	737	1855
R1-113	0.102	0.19	0.18	0.54	0.55	272	800
					Mean value	**519**	**1033**

Uncertainties

The summation of errors arising during the combustion and measuring procedure gives a total error corresponding to 3-20 % of the obtained results above (in Bq/g). For the highest obtained value, 2907 Bq/g, the total error is ± 88 Bq/g (corresponding to 3 %) and for the lowest, 77 Bq/g, the total error is ± 15 Bq/g (corresponding to 20 %).

Since the material within the bulk sample (500-1700 mg) might not be completely homogenous, the results above – determined from sub samples – will only be estimations of the true mean value from each bulk sample. The obtained results from the three different combustions and measurements of R1-058 could be used as a rough estimation of the variations within the same sample. This gives an error of 19 % and 11 %, for the organic and inorganic fraction, respectively.

Discussion

The optimized system proved good performance regarding complete oxidation and complete CO_2 absorption. The system recovery of ^{14}C also appears satisfactory but more thorough investigations would be desirable. This would require graphite samples with known activity to be combusted and measured with LSC.

The conclusion made from the three measurements of sample R1-058 was that the samples were presumed to be inhomogeneous. Because the lack of relevant references, this assumption cannot be verified.

The relevance of measuring background samples has during the experimental procedure proved to be of great importance. During this period the background level (*i.e.* the LSC results from the background samples made of NaOH) has increased about 11 %, which is probably due to the electronics of the liquid scintillation counter.

The investigation clearly shows the importance of continuously monitoring of beta spectra to discover any contaminants. One should also be aware of that the handling of other radionuclides in the laboratory could constitute a potential contamination source.

The summation of the errors arising during the combustion and measuring procedure shows that it is profitable to raise the concentration of activity in the gas washing bottles. This could be accomplished by using larger samples or by precipitating the absorbed CO_2 as carbonate, followed by filtering and washing of the precipitate before analysis. Carbonate precipitation would probably also reduce the problem of contamination of other radionuclides.

A complete separation of organic and inorganic ^{14}C containing compounds in the graphite might be an unrealistic achievement when employing this method. This is a consequence of the definition of organic and inorganic fractions made in the introduction together with the fact that the exact chemical composition of the ^{14}C compounds is not known. The lack of connection between sample and location within the reflector will also introduce an uncertainty, since the measured samples might not be representative for the total amount of graphite. As a result, the obtained data will be an approximation of the true fractions of organic and inorganic ^{14}C-compounds within the graphite. Methods based on sample combustion may therefore be more suitable for measurements of total ^{14}C content. Still, the employed method could be further optimized by combusting ^{14}C-labelled organic and inorganic compounds. Other approaches should however also be considered when aiming at complete separation of the fractions. One approach could involve acid stripping of the sample for determination of the inorganic fraction, followed by combustion to determine the total ^{14}C content (see *e.g.* Stenström *et al.* 2003). The organic fraction is then determined by subtraction.

Acknowledgements

Funding for this project was provided by SKB.

References

Bisplinghoff B, Lochny M, Fachinger J, Brücher H. Radiochemical characterization of graphite from Jülich experimental reactor (AVR). Proc. IAEA Technical Committee Meeting on "Nuclear Graphite Waste Management", 18-20 October 1999, Manchester, UK. TCM-Manchester99. IAEA, 1999.

Bushuev A V et al. Radionuclide characterization of graphite stacks from plutonium production reactors of the Siberian group of chemical enterprises. Proc. IAEA Technical Committee Meeting on "Nuclear Graphite Waste Management", 18-20 October 1999, Manchester, UK. TCM-Manchester99. IAEA, 1999.

Bushuev et al. Quantitative determination of the amount of ^{3}H and ^{14}C in reactor graphite. Atomic Energy 73(6):959-962, 1992.

Greening F R. The characterization of carbon-14 rich deposits formed in the nitrogen annulus gas systems of 500 MWe CANDU reactors. Radiochimica Acta 47:209-217, 1989.

Hollas J M. Modern spectroscopy. 3rd edition. John Wiley & Sons Ltd, 1996.

Magnusson Å. Measurement of the distribution of organic and inorganic ^{14}C in a graphite reflector from a Swedish nuclear reactor. Master thesis. Lund University, NFFR-5016, 2000.

Marsden B J, Hopkinson K L, Wickham A J. The chemical form of carbon-14 within graphite. Report produced for NIREX. SA/RJCB/RD03612001/R01, Issue 4, 2002.

Milton G M, Brown R M. A review of analytical techniques for the determination of carbon-14 in environmental samples. AECL-10803. Atomic Energy of Canada limited, 1993.

Petzold A, Kopp C, Niessner R. The dependence of the specific attenuation cross-section on black carbon mass fraction and particle size. Atmospheric Environment 31(5):661-672, 1997.

Schmid H et al. Results of the "carbon conference" international aerosol carbon round robin test stage I. Atmospheric Environment 35:2111-2121, 2001.

Stenström K, Magnusson Å. Methods of measuring ^{14}C on spent ion exchange resins from nuclear power plants – a literature survey. Internal report, LUNFD6/(NFFR-3090)/1-50(2003), Lund University, 2003.

Stenström K. New applications of ^{14}C measurements at the Lund AMS facility. Doctoral dissertation. Lund University, 1995.

Takahashi R, Toyahara M, Maruki S, Ueda H, Yamamoto T. Investigation of morphology and impurity of nuclear grade graphite, and leaching mechanism of carbon-14. Proc. IAEA Technical Committee Meeting on "Nuclear Graphite Waste Management", 18-20 October 1999, Manchester, UK. TCM-Manchester99. IAEA, 1999.

Study on Photocatalytic Decomposition of Organic C-14 in Waste Packages

H. Asano, K. Kawahara and H. Owada
Radioactive Waste Management Funding and Research Center;
R. Wada, T. Yasunaga, T. Nishimura and T. Nakanishi
Kobe Steel, Ltd.;
Y. Kurimoto
Kobelco Research Institute, Inc.

Introduction

This study focused on the photocatalytic decomposition of organic carbons as one of the treatments of organic C-14 released from radioactive metal wastes. The photocatalytic decomposition of organic carbons, which has already been turned into actual utilizations, is generated by oxidizing species of semiconductors, particularly titanium dioxide (TiO_2), irradiated with ultraviolet (UV). TiO_2 needs the ultra-bandgap energy of UV that has the wavelength less than 388 nm. In this paper, we present a study of the decomposition of organic C-14 by photocatalysts irradiated with β rays of C-14 to evaluate the possibility of photocatalyst applications to treatments of organic C-14 in waste packages.

Objectives

We evaluated the performance and process of the decomposition of organic C-14 using β rays of C-14 with TiO_2.

Experimental

Photocatalysts used during experiments, anatase TiO_2 sintered on cylinder shaped titanium plates are obtained from Kobe Steel, Ltd.

Other studies showed that chemical forms of organic C-14 released from radioactive wastes are acetic acid, formic acid, formaldehyde, methanol and ethanol. In this study, simple C1 organics, C-14 labeled methanol (ICN Biochemicals, #17342), formaldehyde (ICN Biochemicals, #17237) and formic acid (American Radiolabeled Chemicals, #163B), were employed. To prepare test solutions, C-14 labeled regents were diluted with deionized water and the concentration was adjusted to 25 MBq/L ($1.2\text{-}1.4 \times 10^{-5}$ mol/L) in consideration of C-14 inventory after 10,000 years. The solution pH was adjusted to 11 using NaOH simulating alkali condition by cement in repository. The test solutions and photocatalysts were installed and sealed in the glass vials, then they were stored in lead containers for shielding (see Fig. 1). The experiments were carried out at room temperature. The solution samples were taken periodically, inorganic C-14 (carbonate ion) in the solution was separated by carbonate precipitation method. Radioactive concentration of the solution (organic and inorganic C-14), filtrate (organic C-14) and deposit (inorganic C-14) was measured on a liquid scintillation counter to evaluate the decomposition of organic C-14.

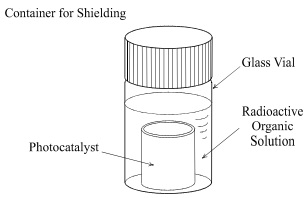

Fig. 1: Schematic of the experiments

Results

Radioactive concentration of C-14 in the methanol solution, filtrate and deposit is shown in Fig. 2. The radioactive concentration of deposit (inorganic C-14) that was not detected at the start of the experiment increased with time, which means methanol was decomposed by photocatalysts irradiated with β ray. The decomposition rate of organic C-14 after 80 days was about 20 %. In addition, the radioactive concentration of filtrate (organic C-14) was decreased rapidly after 20 days. After 60 days, removal rate of organic C-14 reached 90 %, it far exceeded the decomposition rate. On the other hand, the radioactive concentration of methanol solution without the photocatalyst did not decrease, which means there was no effect of evaporation of methanol. Consequently, these results suggest that removal of organic C-14, which exceeds the decomposition of organic C-14, includes adsorption onto surface of the photocatalysts.

Discussion

As described above, it is assumed that the removal rate of organic C-14 includes the adsorption onto the photocatalyst surface. Yamagata et al. [1], [2] proposed that photocatalytic oxidation of methanol occurs on the photocatalyst surface and that most of the intermediates of methanol oxidation are adsorbed onto the photocatalyst surface, where further oxidation to CO_2 takes place (see Fig. 3).

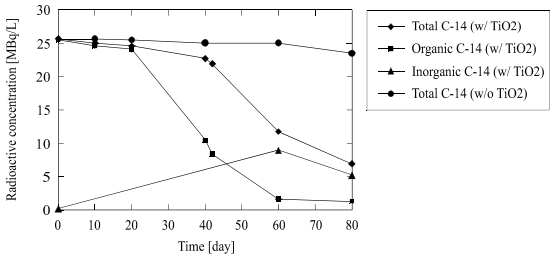

Fig. 2: Radioactive concentration of methanol solution

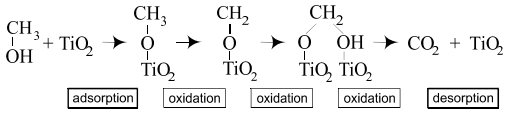

Fig. 3: Proposed decomposition reaction of methanol

Provided the decomposition reaction of methanol follows this reaction path, it is assumed that adsorbed portion would be finally decomposed.

The experiment results of methanol, formaldehyde and formic acid were shown in Fig. 4. The decomposition rate ranged 8-67 % after 75-80 days and the decomposition of these organic carbons by photocatalyst irradiated with β rays is confirmed.

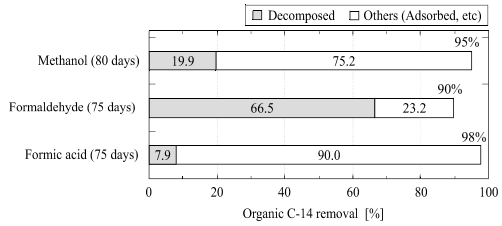

Fig. 4: Decomposition and removal rate of organic C-14

Application to waste packages

In this study, it has indicated that organic C-14 in solution can be decomposed by photocatalysts irradiated with β rays. Therefore, it can be assumed that photocatalysts installed in waste packages could reduce the release of organic C-14 from radioactive wastes. As described above, the decomposition reaction of organic carbons by photocatalysts starts with the adsorption of organic carbons onto the photocatalyst surface. In order to improve the performance of decomposition and removal of organic C-14, it is assumed to be effective to increase the photocatalyst surface area.

At this point, we investigated a method to apply photocatalyst particles as internal filler of waste packages. As shown in Fig. 5, in case nine canisters are placed in a wastes package and the package is filled with photocatalyst particles and ground water flows into it, the total surface area of photocatalyst and the volume of ground water in the waste package are about 1800 m^2 and 0.4 m^3 respectively. The surface area/water volume ratio in this case is about 35 times as much as that in case of the experiments in this study. Provided inside of the wastes package is assumed to be static water environment same as that of the experiment in this study, organic C-14 could be removed in a shorter period.

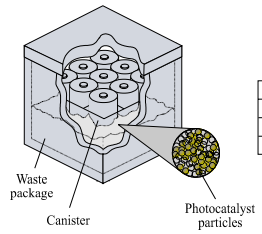

Item	Dimensions
Waste Package	1.45 × 1.45 × 1.45 m
Canister	ø0.43 × 1.34 m × 9
Photocatalysts	ø2 mm Filling factor: 60%

Fig. 5: Installation of photocatalysts in waste packages

Conclusions

We demonstrated the decomposition test of C-14 labeled methanol, formaldehyde and formic acid using TiO_2 photocatalysts. The decomposition of organic C-14 by photocatalysts irradiated with β rays has been clarified. The decomposition rate of the organic C-14 ranged 8-67 % after 75-80 days. In addition, it has been indicated that released organic C-14 could be removed and decomposed in a short period by installing photocatalyst particles in waste packages.

In the future work, the photocatalytic decomposition mechanism including adsorption will be verified, and at the same time, the evaluation of decomposition performance in reduced condition of underground repository sites and effects of components in groundwater (Ca^{2+}, other organic carbons, etc.) are necessary. In addition, since release of organic C-14 occurs after ground water intrudes into the waste packages, long-term performance of photocatalysts needs to be confirmed. Furthermore, it would be necessary to evaluate gas generation of water decomposition by photocatalytic reactions as well as the influences of photocatalytic reactions on corrosion of waste containers and metal wastes.

This paper is a part of the results of "Development of geological disposal techniques" funded by Ministry of Economy, Trade and Industry.

Sadamu Yamagata, Ryo Baba, Akira Fujishima, "Photocatalytic Decomposition of 2-Ethoxyethanol on Titanium Dioxide", Bull. Chem. Soc. Jpn., Vol.62, No.4, pp.1004-1010 (1989).

Jian Chen, David F. Ollis, Wim H. Rulkens, Harry Bruning, "Photocatalyzed Oxidation of Alcohols and Organochlorides in the Presence of Native TiO_2 and Metallized TiO_2 Suspensions. Part (II): Photocatalytic Mechanisms", Water Research, Vol.33, No.3, pp.669-676 (1999).

Fundamental Study of C-14 Chemical Form under Irradiated Condition

K. Noshita, Hitachi

Introduction

In the recent studies, it was found that an activated metal such as zirconium alloy and steel alloy produces low molecular weight of organic C-14 along with a metal corrosion. Due to low sorption abilities of organic C-14, it is very important to evaluate the long-term stability of organic forms.

Generally, an inorganic form is more stable thermodynamically in the disposal condition (pH = 12.5, Eh = -600 mV). However, high energy is required to decompose an organic matter. In this study, irradiation effect was investigated.

Objective

In the actual disposal system, it is possible to expect Nb-94 as a long-term gamma radiation source. This study was carried out to evaluate C-14 chemical form in the waste package considering the radiolysis by Nb-94.

Experimental

In the irradiation experiments, various C-14 isotopes (methanol, formic acid, formaldehyde, ethanol and acetic acid) were used to simulate organic C-14. An alkaline solution (pH=10) and an actual groundwater were used as simulated solutions. The concentration of each solution was adjusted between 10^{-7} mol/L and 10^{-5} mol/L. These samples were irradiated by Co-60 gamma source (0.2 - 200Gy/h) under the anaerobic condition (3 % H_2 gas). After the irradiation, a total C-14 concentration and an organic C-14 concentration were measured to evaluate decomposition ratio and decomposition efficiency as follows:

Decomposition ratio (%) = 100 x $(C_{total} - C_{organic})/C_{total}$

Decomposition efficiency (%) = Decomposition ratio/Irradiation factor

where C_{total} denotes a total C-14 concentration; $C_{organic}$ denotes an organic C-14 concentration; Irradiation factor denotes a theoretical dose necessary for 100 % decomposition of each organic C-14 solution.

Results and Discussion

Organic C-14 may decompose by a direct decomposition and an indirect decomposition by OH radical. In a low organic C-14 concentration, an indirect decomposition is thought to be a dominant process. Decomposition reactions of organic matters should be described as follows.

Formic acid	$HCOOH + 2OH \rightarrow CO_2\uparrow + H_2O$
Formaldehyde	$HCHO + 4OH \rightarrow CO_2\uparrow + 3H_2O$
Methanol	$CH_3OH + 6OH \rightarrow CO_2\uparrow + 5H_2O$
Acetit acid	$CH_3COOH + 8OH \rightarrow CO_2\uparrow + 6H_2O$
Ethanol	$C_2H_5OH + 12OH \rightarrow CO_2\uparrow + 9H_2O$

Firstly, the validity of this model was investigated by a simple irradiation test. Figure 1 shows the experimental results and calculated results. The experimental results agreed with the calculated results obtained by an absorbed energy and G-value. This fact indicates that indirect decomposition model was valid basically.

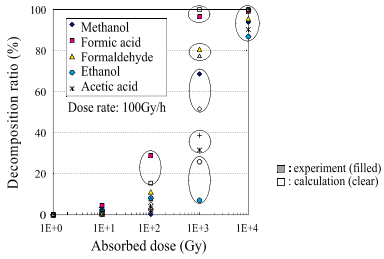

Fig. 1: Comparison of decomposition ratios

Next, the irradiation test was carried out in the simulated conditions of actual disposal system. In the actual system, organic C-14 concentration was determined by various factors such as, concentration of C-14 in activated metal, corrosion rate, surface area, a ratio of organic form and porosity in a waste package. Irradiation conditions were determined by a dose rate, amount of water in the waste package, G-value. Considering these factors, the leaching ratio of Organic C-14 in the waste package was evaluated as 6.6×10^{-9} mol/L/y and theoretical maximum decomposition rate was evaluated as 5.9×10^{-9} mol/L/y. Comparing these values, Organic C-14 becomes almost inorganic, when 1 % of OH radical is consumed for the decomposition.

To investigate the effects of organic C-14 concentration and dose rate on decomposition efficiency, irradiation tests were carried out. Figure 2 shows the effect of organic C-14

concentration on decomposition efficiency. Figure 3 shows the effect of dose rate decomposition efficiency. As a result, the decomposition efficiency increased in proportion to the organic C-14 concentration and the dose rate dependence was not observed in this study.

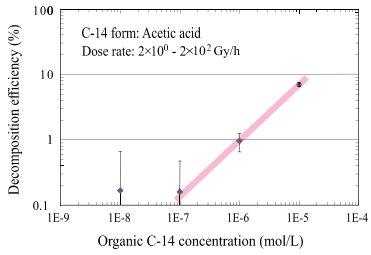

Fig. 2: The effect of organic C-14 concentration on decomposition efficiency

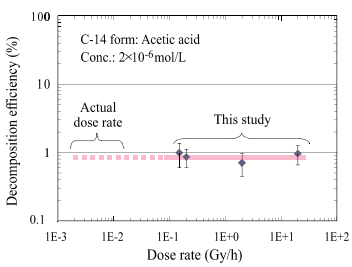

Fig. 3: The effect of dose rate on decomposition efficiency

In the next step, the effects of organic form and groundwater were investigated. Figure 4 shows the effect of organic form on decomposition efficiency. Figure 5 shows the effect of organic form on decomposition efficiency. These results suggest the effects of chemical form and groundwater composition was very small.

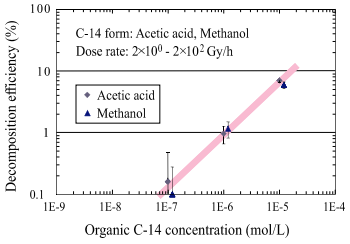

Fig. 4: The effect of organic form on decomposition efficiency

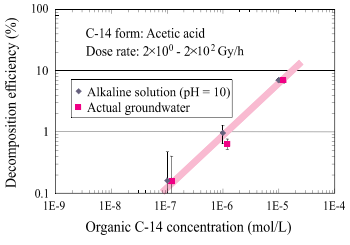

Fig. 5: The effect of organic form on decomposition efficiency

Based on these investigations, it was found that the decomposition efficiency increased in proportion to the organic C-14. This trend suggests that the OH radicals were consumed by the other reactions. That is, the decomposition efficiency was determined by the competitive reaction in the solution. This competition model suggests that the decomposition efficiency should be dependent on the organic C-14 concentration, and the decomposition efficiency is not dependent on dose rate.

To evaluate the irradiation effect, the organic C-14 concentration in the waste package was calculated using a water exchange model. In this water exchange model, we supposed the staying time of C-14 in the waste package. Figure 6 shows a typical calculated result of organic C-14 concentration. This result indicates that the maximum organic C-14 concentration was reduced 10 times considering the irradiation effect.

Based on these investigations, it was found that the effect of radiolysis is very important to evaluate the C-14 chemical form in the actual disposal system.

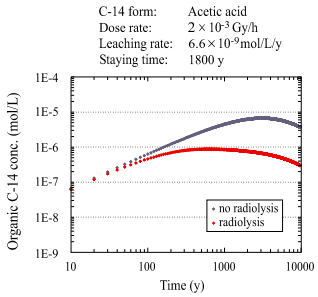

Fig. 6: A typical calculated result of organic C-14 concentration in the waste package

Conclusion

Organic C-14 was decomposed by OH radicals, which were produced by water radiolysis. The decomposition efficiency increased in proportion to the organic C-14 concentration and the dose rate dependence was not observed in this study. The effect of chemical form of organic C-14 and groundwater composition on decomposition efficiency was very small. The decomposition efficiency was determined by the competitive reaction in the solution. This competition model suggests that the decomposition efficiency should be dependent on the organic C-14 concentration, and the decomposition efficiency is not dependent on dose rate. The maximum organic C-14 concentration may reduce 10 times considering the irradiation effect.

In the future work, the effects of competitive substance and low dose rate should be examined. C-14 staying time also should be evaluated considering the waste package design.

Interactions of Carbon in a Repository Environment

B. Kienzler[1], V. Metz[1], M. Kelm[1], C. Nebelung[2] and L. Baraniak[2]

[1] Forschungszentrum Karlsruhe, Institut für Nukleare Entsorgung (INE)
[2] Forschungszentrum Rossendorf, Institut für Radiochemie

Introduction

In the past, some review articles were published covering the production of ^{14}C, required analytical methods, treatment during reprocessing, waste forms, mobilisation, transport and sorption (Bush, 1983; Dayal and Reardon, 1994a; Dayal and Reardon, 1994b). The source term, isolation capacity, and long-term radiological exposure of ^{14}C from the Swedish underground repository for low and intermediate level waste was assessed (Hesboel et al., 1990). Spent ion exchange resins would be the dominant source. Bacterial production of CO_2 and CH_4 from degradation of ion-exchange resins may contribute to the release into the biosphere. Also for Yucca Mountain, ^{14}C source term and consequences of the release are available (van-Konynenburg, 1987).

^{14}C is mainly produced by (n,p) reaction from ^{14}N, at a cross section σ = 1.48 barns for LWR neutron spectrum, and to a less extend by $^{17}O(n,\alpha)^{14}C$, at a cross section of 0.183 barns (Bush, 1983). Important sources of ^{14}C are zircalloy cladding (according ASTM standard N: max. 65 ppm) and spent fuel (N contamination and the content of 0.038 % of ^{17}O). Additionally, activation of the coolant or the moderator contributes ^{14}C to some extent. An estimation of the production of ^{14}C in LWR is presented by (Bleier et al., 1987): In the gas plenum of the studied fuel elements of PWR and BWR a negligible concentration of ^{14}C was found. In BWR waste, the ^{14}C concentration of spent fuel (22000 MWd/t) was 7000 Bq/g UO_2, and the ^{14}C concentration of the cladding was 22600 Bq/g zircalloy. In spent fuel of a 30000 MWd/t PWR a ^{14}C concentration of 9300 Bq/g UO_2 was determined. PWR cladding was not investigated. A correlation of the ^{14}C production with the burn-up was obtained to be 370 - 390 GBq ^{14}C per (GWe·yr). After reprocessing and dissolution of spent fuel in concentrated HNO_3 more than 99.0 % of ^{14}C is found in $^{14}CO_2$. The remaining ^{14}C content is bound to various compounds, such as ^{14}CO, $^{14}CH_4$.

In Germany, organic materials containing ^{14}C markers, metals containing ^{14}C as carbides and other low level waste forms containing ^{14}C in carbonates or in ashes are important ^{14}C sources. Spent fuel elements from pebble bed HTRs[1] having a graphite matrix contribute to the total ^{14}C load to a less extent (Rainer and Fachinger, 1998).

[1] High Temperature Reactors

Treatment and behaviour of ^{14}C loaded waste

During HTR operation in Germany a total ^{14}C inventory of $5x10^{12}$ Bq was generated which is incorporated in 675000 fuel spheres. Studies on interactions of spent HTR fuel with brines show that ^{14}C in graphite from these fuel elements is almost immobile. For the duration of interim storage, the graphite may be oxidized to some extent due to the gamma radiation and contact with air, resulting in generation of $^{14}CO_2$ release. When the oxygen content of the storage canisters, containing 950 fuel elements each, is completely consumed, less than 2 % of the ^{14}C inventory can be oxidized (Niephaus et al., 1997; Rainer and Fachinger, 1998).

The release of ^{14}C from zircalloy hulls from LWR fuel was studied by Kaneko (Kaneko et al., 2002). Usung water as leachant, both organic and inorganic species were found. The released fraction increased with time and pH. To get a better understanding of the mechanisms involved, tests were performed using ZrC and Fe$_3$C and mixtures of carbon with metals. Organic species (carboxylic acids, formaldehyde, methanole and ethanole) were detected only in the case of carbides. The concentrations of leached organic carbon (DOC) from carbides were about twice of the dissolved inorganic carbon (DIC). Comparing the findings indicate that ^{14}C exists mainly in carbides in irradiated zircalloy.

Other waste forms may release ^{14}C in a large variety of inorganic and organic species. Inorganic waste forms from ^{14}C production, mainly Al-carbides, are disposed of in the Morsleben repository, ERAM in Germany (amounts are not published). Reactions of carbides with water/brine may produce methane or acetylene gas. Organic waste forms bearing ^{14}C can be transformed into gaseous $^{14}CO_2$ and $^{14}CH_4$ due to microbial reactions.

Conditioning of organic ^{14}C bearing materials is of high importance. At Forschungszentrum Rossendorf (FZR), for save disposal of large variety of ^{14}C labelled organic materials[2] a process and corresponding apparatus were developed and applied. A photocatalytic oxidation step decomposes the ^{14}C-labeled compounds by means of TiO_2 and UV irradiation. Resulting $^{14}CO_2$ is dissolved in NaOH and reacts with $BaCl_2$ forming slightly soluble barium carbonate ($BaCO_3$). (FZR, Annual Reports 1998 and 1999).

In the long term, biodegradation of organics in a repository may occur. Unprocessed organic ^{14}C-containing materials will undergo the same reactions. Depending on pH, and the availability of different electron acceptors (O_2, NO_3^-, Fe^{3+}, SO_4^{2-}, CO_2) different reactions may take place (Jones and Atkins, 1991). (CH_2O represents one unit of a cellulose molecule.)

$>CH_2O + O_2$	$\rightarrow CO_2 + H_2O$	ΔG°=-502.4 kJ mol^{-1}
$>CH_2O + 4/5\ NO_3 + 4/5\ H^+$	$\rightarrow CO_2 + 2/5\ N_2 + 7/5\ H_2O$	ΔG°=-476.9 kJ mol^{-1}
$>CH_2O + 8\ H^+ + 4\ Fe(OH)_3$	$\rightarrow CO_2 + 11\ H_2O + 4\ Fe^{2+}$	ΔG°=-116.0 kJ mol^{-1}
$>CH_2O + ½\ CO_2$	$\rightarrow CO_2 + ½\ CH_4$	ΔG°=-92.9 kJ mol^{-1}

In the presence of both nitrate, a degradation of the organic materials such as cellulose has to be expected mainly by denitrification. End-products are CO_2, HCO_3^-, CO_3^{2-} which exist in equilibrium corresponding on the actual geochemical conditions. Therefore, release and migration of ^{14}C cannot be treated independently from the bulk of inorganic and organic carbon waste components in a repository.

[2] For tests of the process, 4-hydroxy benzoic acid and acetic acid were applied.

Experimental investigation on the release of ^{14}C from wastes

At WIPP, a Mg bearing backfill material (periclase, MgO) is added to the waste in order to keep the concentration of HCO_3^-/CO_3^{2-} at a minimum by formation of solid carbonate phases (Brush et al., 2002). Limiting the concentrations of (bi-)carbonates in solution results also in a low actinide solubility, especially at high pH. At FZK-INE and FZR, various experimental and theoretical investigations have been performed in order to quantify the release of ^{14}C. The experiments were performed in concentrated salt solutions.

For the Asse salt mine, a $Mg(OH)_2$-based backfill material was proposed by FZK-INE (Schuessler et al., 2001). This material consists mainly of brucite ($Mg(OH)_2$(cr)) and a Mg-oxychloride type solid ($Mg_{2x}(OH)_{2x-1}Cl{\cdot}4H_2O$(s)) (Metz et al., 2003). In order to improve the thermodynamic database of the main constituents, solid-liquid equilibria of $Mg(OH)_2$(cr) and pure Mg-oxychloride $Mg(OH)_2Cl{\cdot}4H_2O$(cr) were determined in the system Mg-Na-OH-Cl-H_2O (Altmaier et al., 2003). Various experimental and modelling studies were carried out to determine the stability of the $Mg(OH)_2$-based material in the relevant brines, formation of secondary phases, and the effect of the material on actinide solubility in case of carbonate-input to the brines. After exposition of the backfill material to CO_2 gas in an autoclave for 5 months, the formation of magnesite and magnesium-hydroxo-carbonate are identified (Fig. 1).

For the ERAM system, sorption of $^{14}CO_3^{2-}$ onto salt concrete, sorel concrete and "Grauer Salzton" (natural conglomerate of rock salt and clay phases) was investigated. The experiments were performed in NaCl brines equilibrated with the sorbens (pH 9 for sorel material and pH 10.6 for salt concrete, respectively) and $MgCl_2$-rich brines equilibrated with the sorbens (pH 6 to 6.7). The solubility of ^{14}C species in the presence of ^{14}C containing $BaCO_3$ ($1x10^{-2}$ mol/l) is $6x10^{-3}$ mol/l - $1x10^{-2}$ mol/l in $MgCl_2$-rich brine, and $3x10^{-5}$ mol/l - $9x10^{-4}$ mol/l in NaCl brine.

For all materials under investigation, sorption showed distinct time dependences. Strong sorption was detected for $^{14}CO_3^{2-}$ in NaCl solution onto sorel concrete (R_s ~ 3000 ml/g), salt concrete (Rs ~ 600 ml/g) and in $MgCl_2$-rich brine onto sorel concrete (Rs ~ 1200 ml/g). Almost insignificant sorption of carbonate onto salt concrete was found in $MgCl_2$-rich brine (R_s = 2.6 ml/g to 2.9 ml/g) and onto "Grauer Salzton" in all brines (R_s = 2.5 ml/g to 8,2 ml/g). Dissolved carbonate in the conditioned solutions used for the experiments were determined between $1.8x10^{-3}$ mol/l and $7.3x10^{-3}$ mol/l in $MgCl_2$-rich brine, and between $6.1x10^{-5}$ mol/l and $1.3x10^{-4}$ mol/l for NaCl brine. Sorption data can be explained by assuming isotopic exchange between dissolved ^{14}C-carbonate and inactive carbonates. Observed retention coefficients in the NaCl systems agree well with published data for Portland cement, e.g. (Dayal and Reardon, 1994b; Noshita et al., 1996).

^{14}C sorption studies were performed for Konrad specific systems, also (Zhang, 1993). These systems cover a lower cretaceous host rocks and cemented waste forms. The distribution coefficients between inorganic and organic carbon (saccharose) were measured in the range of $1\text{-}8x10^3$ ml g^{-1}.

Sorption was also studied in Konrad, Asse and Gorleben far-field systems. The distribution coefficients were found to be in the range of 0.06 to 0.2 ml g^{-1} for saline Asse and Gorleben systems, and 0.7 to 2.0 ml g^{-1} for cohesive rocks (Bode and Wolfrum, 1989; Wolfrum et al., 1988).

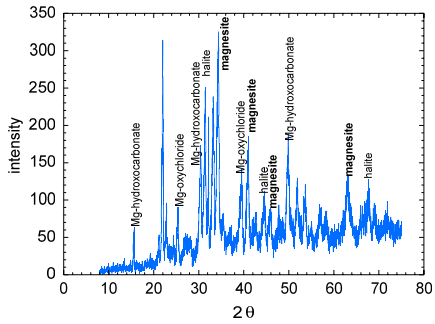

Fig. 1: X-ray diffractogram showing the formation of carbonates in autoclave experiment

Sorption of methane under near-field conditions

The tests were performed by monitoring the concentration of gaseous CH_4 in a mixture with a noble gas (Ar) which does not react with slurry components. Sorption of methane (CH_4) onto the backfill materials ($MgCl_2$-rich brine - sorel systems) was investigated by contacting a brine /backfill slurry with the gas. First, the samples were homogenized; then, the test vessels (gas volume 200 ml, solid/brine system 50 ml) flushed by argon to replace remaining air and evacuated. After double evacuation, a methane/Ar mixture (Prüfgas Methan Ar 55.3/44.7) was added (300 und 450 hPa). The composition of the gas mixture was chosen that no change of the gas composition had to be expected by gas sorption / dissolution processes. For a period of one week, the vessels were stored and shaken. Sampling was performed in an evacuated sampling system.

The analysis of experimental results shows that the ratio of CH_4/Ar remains constant within a deviation of 5 %. Consequently, the total methane sorption onto the studied backfill materials remains below 0.2 mmol CH_4/kg solid material.

Modelling exercise

In the Asse salt mine, low- and intermediate-level radioactive waste was emplaced in a depth of about 750 m and 511 m below ground from 1967 to 1978. The backfill concept have to guarantee i) long-term geochemical stability in case of brine access and ii) geochemical buffering of the solution with respect to pH, Eh and pCO_2. The modelling procedure is described in (Metz et al., 2003). For modelling, the inventories of waste matrix and backfill materials as well as the different waste components were normalized with respect to the volume of penetrating Q-brine (per kg H_2O). For these normalized inventories, reaction path modelling

was performed by means of the thermodynamic equilibrium code EQ3NR/EQ6 (Wolery, 1992). Thermodynamic activities and interactions of dissolved species were calculated using the Pitzer formalism (Pitzer, 1979) and an extended Pitzer-Harvie-Møller-Weare data base (Harvie et al., 1984). For modelling of cement systems, silicate and aluminate species as well as additional solid phases were incorporated into the data base.

Modelling results show that in case of brine access to the emplacement rooms in the absence of buffering materials, the geochemical milieu is mainly controlled by corrosion of Portland cement and degradation of organic materials. *Organic waste* is present in the emplacement rooms in different forms such as cellulose, plastic materials, and laboratory wastes. Due to the fact that a high load of nitrate is present in the waste forms, it cannot be excluded that considerable amounts of the organic carbon inventory will be degraded to CO_2 by halophilic bacteria. Therefore, a complete transformation of the organic carbon inventory into inorganic carbon is assumed as one limiting case for performance assessment. The inorganic carbon species react with dissolved cations, solution constituents and radionuclides, forming dissolved and solid species. In some of the emplacement rooms a high inventory of carbon relative to the inventory of cement was emplaced. Here, acidification (pH < 4) in case of total conversion to DIC and CO_2(g) is expected.

Backfilling of the emplacement rooms by Portland cement or crushed rock salt results in an increase of the respective cement/brine ratio. In order to buffer the brine-solid system in the preferred pH-range and to keep carbonate concentration low in the emplacement room, the $Mg(OH)_2$-based backfill material should be used. Thermodynamic calculations show that in the presence of the backfill material under investigation, the CO_3^{2-} concentration is limited by (Ca,Mg)-carbonate precipitation to values below 10^{-6} mol (kg H_2O)$^{-1}$. For a sufficient supply of the $Mg(OH)_2$-based material, the pH is buffered to values around 8.5 even for relatively high cement/brine ratios.

Summary and conclusions

- In a repository, ^{14}C load arises mainly from irradiated materials, spent fuel and organic tracers.
- The release of ^{14}C during storage of THTR spent fuel is influenced by contact with air and gamma radiation generating CO_2.
- In a repository in rock salt, dissolved carbonate species sorb onto carbonate containing solids by isotopic exchange.
- In cement dominated systems, rather high distribution coefficient between DIC and DOC is observed (>1000 ml g^{-1}).
- By interaction of CO_2 gas with Mg bearing backfill/buffer material, formation of magnesite and magnesium-hydroxo-carbonate is observed.
- Weak sorption of $^{14}CO_3^{2-}$ onto salt concrete occurs in $MgCl_2$-rich brine. Sorel phases reduced the dissolved ^{14}C concentration by more than 2 orders of magnitude during a 1 yr. period.
- Sorption of methane onto solids could not be verified.

Experimental findings are in agreement with the modelling predictions. By taking into account an isotopic exchange the gaseous and dissolved ^{14}C concentrations are controlled by precipitation of solids.

Acknowledgement

Parts of the work were financially supported by the Bundesamt für Strahlenschutz (BfS) and by the Forschungsbergwerk Asse.

References

Altmaier, M., Metz, V., Neck, V., Müller, R. and Fanghänel, T., 2003. Solid-liquid equilibria of Mg(OH)2(cr) and Mg2(OH)3Cl4H2O(cr) in the system Mg-Na-H-OH-Cl-H2O at 25 °C, pp. 21.

Bleier, A., Kroebel, R., Neeb, K.H. and Wiese, H.W., 1987. Kohlenstoff-14 in LWR-Brennstäben und dessen Verhalten beim Wiederaufarbeitungsprozess, Jahrestagung Kerntechnik '87. Kerntechnische Gesellschaft e.V., Karlsruhe, pp. 417-420.

Bode, W. and Wolfrum, C., 1989. Retardation of dissolved radionuclides in consolidated sedimentary rocks. The influence of MgCl2 brine, Water-Rock Interaction, Miles.

Brush, L.H., Snider, A.C., Bryan, C.R. and Wang, Y., 2002. The use of magnesium oxide as an engineered barrier in the WIPP, Trans. 6 Int. Workshop on Design and Construction of the Final Repositories: Backfilling in Radioactive Waste Disposal,, Brussels.

Bush, R.P., 1983. Carbon-14 Waste Management. A review, International Conference on Radioactive Waste Management. IAEA, Seattle.

Dayal, R. and Reardon, E.J., 1994a. Carbon-14 behaviour in a cement-dominated environment: Impacts for spent Candu resin waste disposal. Waste Management, 14(5): 457-466.

Dayal, R. and Reardon, E.J., 1994b. Cement-based engineered barriers for carbon-14 isolation. Waste Management, 12: 189-200.

Harvie, C.E., Moller, N. and Weare, J.H., 1984. The prediction of mineral solubilities in natural waters: The Na-K-Mg-Ca-H-Cl-SO_4-OH-HCO_3-CO_3-CO_2-H_2O system to high ionic strengths at 25 °C. Geochimica and Cosmochimica Acta, 48: 723-751.

Hesboel, R., Puigdomenech, I. and Evans, S., 1990. Source terms; isolation and radiological consequences of carbon-14 waste in the Swedish SFR repository. SKB TR--90-02, Stockholm.

Jones, M.A. and Atkins, W.S., 1991. Gas generation in deep radioactive waste repositories: A review of processes, controls and models. DOE-HMIP-RR 90/0986.

Kaneko, S. et al., 2002. A Study on the Chemical Forms and Migration Behavior of Carbon-14 Leached from the Simulated Hull Waste in the Underground Condition, Scientific Basis of Nuclear Waste Management, Boston.

Metz, V., Schüßler, W., Vejmelka, P., Lützenkirchen, J. and Kienzler, B., 2003. Radionuclide source term for the Asse salt mine – geochemical assessment for the use of magnesium(II) based backfill material, The 9th International Conference on Radioactive Waste Management and Environmental Remediation, Oxford, UK.

Niephaus, D., Storch, S. and Halaszovich, S., 1997. Experience with the interim storage of spent HTR fuel elements and a view to necessary measures for the final disposal. IAEA-TECDOC--1043, IAEA, Vienna.

Noshita, K., Nishi, T., Matsuda, M. and Izumida, T., 1996. Sorption of carbon-14 by hardened cement paste, Mat. Res. Soc. Proc., pp. 435-442.

Pitzer, K.S., 1979. Theory: Ion interaction Approach. In: R.M. Pytkowicz (Editor), Activity coefficients in electrolyte solutions. CRC Press, INC. Boca Raton Fl., pp. 157-208.

Rainer, H. and Fachinger, J., 1998. Studies on the long-term behaviour of HTR fuel elements in highly concentrated repository-relevant brines. Radiochimica Acta, 80: 139-145.

Schuessler, W., Kienzler, B., Wilhelm, S., Neck, V. and Kim, J.I., 2001. Modelling of near field actinide concentrations in radioactive waste repositories in salt formations: Effect of buffer materials. Mat. Res. Soc. Symp. Proc, 663: 791-798.

van-Konynenburg, R.A.S., C.F.; Culham, H.W.; Smith, H.D., 1987. Carbon-14 in waste packages for spent fuel in a tuff repository., Scientific basis for Nuclear Waste Management X. . Materials Research Society., Pittsburgh, PA (USA). pp. p. 185-196.

Wolery, T.J., 1992. EQ3NR, A computer program for geochemical aqueous speciation-solubility calculations: Theoretical Manual, User's guide and related documentation(Version 7.0), UCRL-MA-110662 PT III.

Wolfrum, C., Klotz, D. and Bode, W., 1988. Bestimmung des Sorptions-/Desorptions-verhaltens aus gewählter Radionuklide an Sedimentgesteinsproben des Asse-Deckgebirges. GSF-Bericht 25/88, GSF.

Zhang, Z.X., 1993. Study for establishing proof of the long-term safety of ultimate disposal of spent HTR fuel elements in an underground repository embedded in rock strata. Juel-2796, Forschungszentrum Juelich GmbH (Germany). Inst. fuer Chemische Technologie.

Study on Chemical Behavior of Organic C-14 under alkaline condition

M. Sasoh, Toshiba

Introduction

It was confirmed from some experiments that the organic C-14 generated from activated metals in alkaline solution. If the carbon in metallic matrix is carbide, it is thought that the generation of organics in the leaching solution causes from carbides reaction with water such as hydrolysis of zirconium carbide. In the case of atomic carbon, the organic carbon species should result from the reduction of carbon with oxidizing metal to ist oxides. Figure 1 shows the Eh-pH Diagram for C and Zr, and the condition for disposal site. There is possibility to oxidize from organic carbon to inorganic in the disposal environment.

Objective

From leaching experiments, organic carbon species were identified as low-molecular weight alcohols, carboxylic acids and aldehydes. The identified carboxylic acids were formic acid (HCOOH) and acetic acid (CH_3COOH) from HPLC, and the aldehyde was formaldehyde (HCHO). Methanol (CH_3OH) and ethanol (C_2H_5OH) were confirmed in the Liquid Chromatograms (HPLC). We investigate the stabilities of these organic carbon species in disposal condition.

Experiment

In this study, two types of solution were prepared. The activated stainless steel from the reactor was cut in pieces were leached in alkaline solution, contacted with CSH gel (Ca/Si=0.65) previously. To leach C-14 from the activated metallic phase, these samples were kept under reducing atmosphere for one month. After the metallic phase was separated by filtration, Co-60 was removed form the solution with cation exchange to avoid the radiolysis. Sampling of the solutions was conducted at regular intervals, and the concentrations of organic C-14 and inorganic C-14 were measured using some chemical procedure and β ray counting. High performance liquid chromatography (HPLC) following the β ray counting was also carried out for the solution samples to identify the organic carbon compounds and their concentrations.

For the each chemical forms degradation in the solution, the alkaline solution added the one chemical was used in this study. These samples were kept in a glove box under reducing atmosphere. Sampling of the solutions was conducted at regular intervals, and the concentrations of total carbon, organic carbon and inorganic carbon were measured using a continuous total organic carbon analyzer.

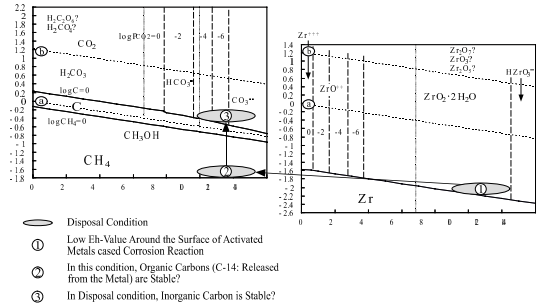

Fig. 1: Eh-pH Diagram for C and Zr, and the condition for disposal site

Results

Figure 2 shows the change of the ratio for organic carbon and the change of the ratio for each organics in total organic carbon from the experiments with activated metal. The released organic C-14 concentration from the activated metals decreased gradually. From the HPLC following the β ray counting acetic acid was most decomposed compound in the organic carbons detected.

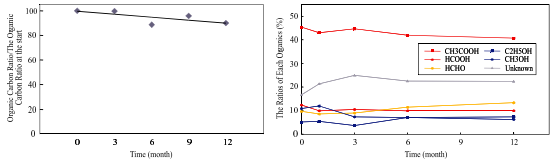

Fig. 2: The change of the ratio for organic carbon and the change of the ratio for each organics in total organic carbon from the experiments with activated metal

Table 1 shows the ratio of residual organic carbon in the each solution after 14 months. In the higher pH Condition, the rate for the change to inorganic carbon might be faster.

Tab. 1: The ratio of Residual Organic Carbon in the Solution of Each Experiment after 14 months

Added Organics		The Residual Ration (After 14 months)	
		pH 8	pH 12.5
Carboxylic Acid	Formic Acid	88 %	71 %
	Acetic Acid	91 %	84 %
Aldehyde	Formaldehyde	90 %	80 %
	Acetaldehyde	90 %	77 %
Alcohol	Methanol	90 %	73 %
	Ethanol	88 %	72 %

Discussion

From these experiments, the organic carbon compounds would be decomposed to in organic carbon in alkaline and reduced condition. The residual organic compound depends on the pH of solution in each experiment, so it would be thought that the hydrolysis in alkaline solution caused the organic compound decomposition. The acetic acid decomposition was more effective than another, but organic carbon might change slowly.

Summary

In the repository site the organic carbon might be decomposed to inorganic compound from this study. We are going to study for reaction of hydrolysis for organic C-14 in alkaline condition and reaction velocity of this hydrolysis. If the hydrolysis for organic C-14 in alkaline condition is occurred in disposal site, the rationalization will achieve in engineering for disposal facility.

Investigations of Distribution Coefficients for C-14 from Activated Metal

M. Sasoh, Toshiba

Introduction

In the performance assessment of transuranic (TRU) waste disposal, from the Nuclear Fuel Reprocessing Facility and MOX fuel facility, carbon-14 (C-14) in the hull (activated zirconium alloy cladding waste) and end pieces has been so far estimated to considerably contribute to the radiation exposure to the public, shown following I-1291). In this performance assessment, however, the estimation is based on the fairly conservatively selected parameters for C-14, since the chemical forms of C-14 leaching from the hull are unknown.

Objective

The distribution coefficients (Kd-Value) of cements for C-14 released from activated metal were measured in this study. For another types of materials that would be suitable for engineering barrier, the distribution coefficients experiments were carried out in this study, too.

Experimental Procedure

For the experimental using activated metals, the experimental solution was prepared by leaching of the hulls and activated stainless steel in the simulated ground water. OPC and Mixed Cement, blast furnace slag is 90 % and OPC is 10 %, were contact with experimental solution.

The simulated ground water, which was contacted with CSH gel (Ca:Si=0.65), were used in activated metals. These samples were kept under the reducing atmosphere.

For the investigation of the C-14 sorption of another materials, the solution added the organic compounds spiked C-14 was used. In this case, carboxylic acids were main chemical forms in these experiments.

The liquid solid ratio was 1g/10ml in all experiments were carried in the reduced atmosphere for a week. Liquid scintillation analyzer was used for measurements of C-14 in the experimental solution.

Results

Table 1 shows the Kd-Values of cements for C-14 from the hulls reaching experiments, and Table 2 was the results for C-14 from the activated stainless steel. In some of the case for the stainless steel experiment, Co-60 was removed from the solution with cation exchange method before the sorption experiments, too. The Kd-Values for C-14 from these experiments were smaller than that of carbonate.

Tab. 1: The Kd-Values of cements for C-14 from the hulls (ml/g)

Cement	RUN No.	Metallic Sample	Sample covered with Zirconium Oxide	Ave.
OPC	1	1.9	5.8	—
	2	4.6	2.5	—
	Ave.	3.3	4.2	3.7
Mixed cement	1	3.6	3.6	—
	2	2.7	8.8	—
	Ave.	3.2	6.2	4.7

Tab. 2: The Kd-Values of cements for C-14 from the activated stainless steel (ml/g)

項目			RUNA	RUNB					Ave.
Leaching Time			11Months	1 Months					–
Setting Time			0 Month	0 Month	1Month	3 Months	6 Months	12 Months	Ave.	–
Th Ra io for TOC(C-14)			37%	74.9%	74.6%	66.2%	71.6%	67.3%	–	–
Cement	OPC	Inorg.	580	245	486	1060	873	870	707	686
		Org.	7.5	9.3	5.8	3.5	5.9	2.9	5.5	5.8
		Total	35	15	11	10	12	9.1	11.4	15.4
	Mixed Cement	Inorg.	90	–	–	–	–	–	–	–
		Org.	12	–	–	–	–	–	–	–
		Total	33	–	–	–	–	–	–	–

Table 3 shows the Kd-Values of several materials for each carbon compounds. Carboxylic acids were sorbed on the materials without illite effectively. The synthetic halloysite has higher Kd-Value than that of OPC from the experiments.

Tab. 3: The Kd-Values of several materials for each organic carbon compounds (ml/g)

Materials	Oraganic Carbon Compounds				
	Acetic Acid	Formic Acid	Formaldehyde	Methanol	Ethanol
Ettringgite	7.3	16	6	0.4	
Hydrotalcite	14	21	7	0.4	
Illite	5.9	0.1	3.8	1.2	8.4
Japanese Acid Clay	39	7	3.2	0.5	13
Halloysite	65	15	3.8	0.3	12
Chacoal	20	11	43	2.5	17

Discussion

The difference for Kd-Values for the kind of cement materials, OPC and mixed cement wasn't obviously appeared in the experiments with activated metals. The CSH gel includes high concentration of Ca (Ca/Si=1.8) in hydrated OPC, for mixed cement used in this study, its CSH gel has lower concentration of Ca (Ca/Si=0.9). It think that the Kd-Values of CSH gels for organic C-14 are similar to each other type of CSH gel's The synthetic halloysite was effective to adsorb for organic C-14, but another investigation might needs for the engineering barrier.

The correlation of the Kd-Value from the experiments with activated metals and that for spiked compounds experiments wasn't clear in this study. It caused that the concentration for each organic compound, ion strength was not same in these experiments.

Summary

The Cement Kd-Values for C-14 from activated zirconium alloy (hulls) and activated stainless steel were measured in this study. For further investigation of organic C-14 sorption from the activated metal would need another study. The Kd-Values database preparedness for some organic carbon, for example carboxylic acids and Alcohols, and Inorganic Carbon would be very important for setting up to the C-14 in the activated metals.

C-14 Source Term Characterisation and Migration Behaviour of C-14 Labelled Bicarbonate in Boom Clay

D. Boulanger, Belgonucleaire
R. Gens, A. Dierckx and H. Van Humbeeck, Ondraf/Niras,
P. De Cannière, SCK·CEN

Though the small amounts of ^{14}C produced during operation of LWRs are not relevant as regards their radioactivity balance, it is of definite interest with respect to the final disposal of the spent fuel.

As a first step in the performance assessment study on spent fuel it is important to evaluate the inventory and chemical state of ^{14}C in the irradiated assembly, and more particularly, in the fuel rod, which is the purpose of the present work.

^{14}C production

The production of ^{14}C during irradiation of the fuel assembly is mainly attributable to the following major nuclear reactions:

- ^{14}N (n,p) ^{14}C (^{14}N abundance in natural nitrogen is 99.63 %)
- ^{17}O (n,α) ^{14}C (^{17}O abundance in natural oxygen is 0.038 %)
- Ternary fission product

Because of its low content and low isotopic abundance, the ^{13}C neutron capture gives a negligible contribution to the total production of ^{14}C in LWRs.

N and O are included in the composition of the as-fabricated fuel rod and their contents can be defined as follows:

Nitrogen

The nitrogen content of the as-fabricated UO_2 and MOX fuel pellet is typically of a few wt.ppm (up to a few tens wt.ppm have been measured [1]).

The ANSI/ASTM Standard Specification C776 limits the N concentration in the sintered UO_2 pellet to 75 wt.ppm.

Comparably, as regards the zircaloy cladding of the fuel rods, the as-fabricated measured contents range typically between a few wt.ppm and a few tens wt. ppm.

The ANSI/ASTM Standard Specification B353 limits the N concentration in zirconium alloy tubes for reactor service to 80 wt.ppm.

For what concerns the stainless steel spring included in the plenum of the fuel rod, the specifications on maximum allowed content is of the order of 0.1 wt.% (ASME Standard SA-240 mentions 0.1wt.% for 304 stainless steel).

Oxygen

The oxide fuel is of course the major oxygen source of the fuel rod (stoichiometric UO_2 has an oxygen content of 11.8 %).

The as-measured oxygen contained in the zircaloy cladding is typically below 1500 wt.ppm.

Calculations were performed [2] on the ^{14}C production in both the active and the non-active parts of typical UO_2 and MOX fuel assemblies loaded in the Belgian PWR reactors.

The nitrogen contents used as calculation input were set to :

- either 30 or 75 wt.ppm for the fuel,
- 80 wt.ppm for Zircaloy,
- either zero or 800 or 1000 wt.ppm for stainless steel,

and correspond to specification limits of the related fabrications.

As mentioned above, measurements of nitrogen content on as-fabricated fuel pellets and cladding tubes confirm that true contents are of the same order of magnitude as the specification limits.

The ^{14}C masses were calculated (contents at end of irradiation):

- For the active part, with ORIGEN-2, using burnup-dependent libraries generated by the assembly code CASMO,
- For the non-active part, with the Monte Carlo code MCBEND.

Fig. 1 shows the amount of ^{14}C produced in the fuel rods, as compared to the total assembly production.

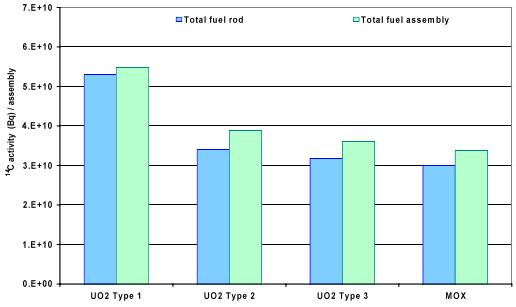

Fig. 1: Calculated ^{14}C production in PWR fuel assemblies: Fraction of ^{14}C in the fuel rods

The fuel rod is roughly composed of 80 wt% fuel and 20 wt% Zircaloy (the stainless steel springs represents less than 1 wt% of the rod).

Fig. 2 gives the calculated productions in the fuel rods of four PWR assembly types (three UO_2, one MOX) differing in geometry, composition and power history.

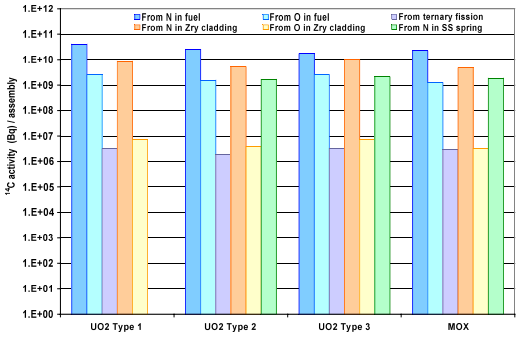

Fig. 2: ^{14}C production in PWR fuel rod: Analysis of the major production modes

Fig. 3 details the major productions relatively to the total mass of the fuel rods in the assembly, as a function of the burnup and impurity input.

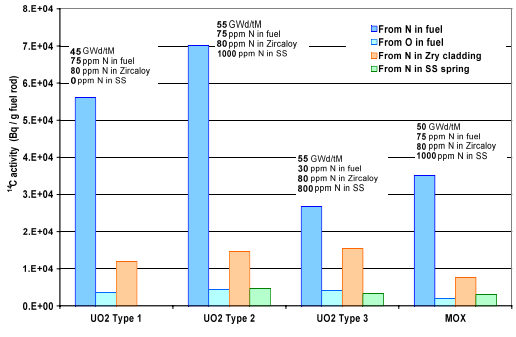

Fig. 3: ^{14}C production in PWR fuel rod: Impact of fuel type and impurity content

Figs. 1 to 3 allow the following main observations:

- About 90 % of the total production is related to the fuel rods (i.e. fuel, cladding and spring); the other structural parts (nozzles, grids,…) thus contribute to the remaining 10 %.
- Nitrogen impurity content in fuel and cladding is of major importance for the production of ^{14}C (productions by ternary fission and oxygen impurity in Zircaloy correspond to less than 0.1 % of the total ^{14}C activity).
- For similar burnup and nitrogen impurity contents, the ^{14}C production in MOX fuel is about half of that in UO_2 fuel.

Fig. 4 shows the comparison of various PWR calculations of ^{14}C production in the fuel (including the above work) with the mention, when available, of the considered as-fabricated nitrogen impurity content of the fuel [3 to 6].

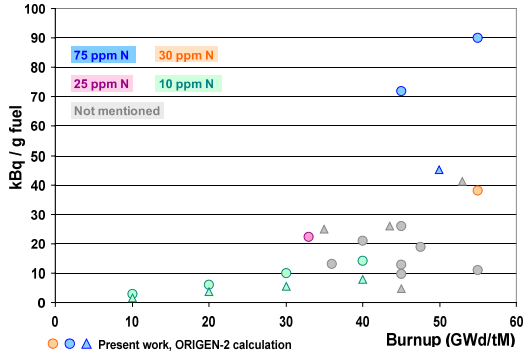

Fig. 4: ^{14}C production in PWR fuel: Various calculation results for UO_2 and MOX fuels

One notes the good consistency of all these calculated data, also confirming the lower ^{14}C production for MOX compared to UO_2 PWR fuel (calculations with 10 wt.ppm initial nitrogen content, [3]).

Fig. 5 compares the calculated values with known initial nitrogen content to various measured ^{14}C contents in irradiated fuel samples [3, 7 to 11]. The experimental values range between 3 and 35 kBq / g fuel, which is very consistent with calculated data and tends to indicate that at least a significant fraction of the ^{14}C production is retained in the fuel.

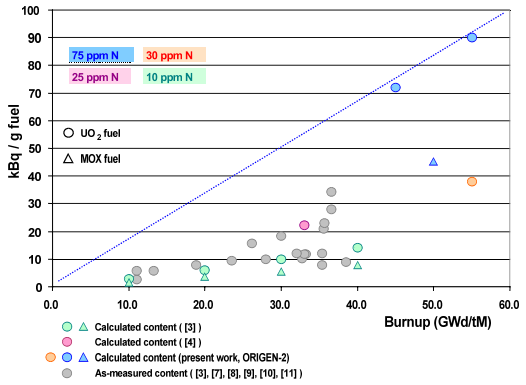

Fig. 5: ^{14}C production in PWR fuel: Calculation and measurements data

Fig. 6 shows the results of various calculations and measurements of ^{14}C in the zircaloy cladding (including the above work) with the mention, for the calculations, of the considered as-fabricated nitrogen impurity content of the cladding [3,7,10,11].

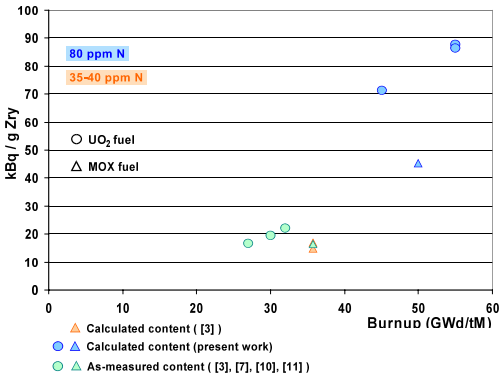

Fig. 6: ^{14}C production in the Zircaloy cladding of a PWR fuel rod: Comparison between calculations and measurements

^{14}C distribution and chemical form in the fuel rod

As fabricated UO_2 and MOX fuels contain nitrogen impurity mainly as a result of the UO_2 powder fabrication process.

The first industrial process, developed in the United States around 1950 and widely used, consists in the UF_6 conversion to uranyl nitrate, then precipitated as ammonium di-uranate (ADU process), followed by its decomposition to UO_3 and further reduction to UO_2.

An important and simpler alternative to this process was developed in Germany around 1960 : preparation of ammonium uranyl carbonate (AUC process), decomposed to UO_3 and then reduced to UO_2.

One notes that the third and last process used at industrial scale was developed in Great Britain in the years 70 and consist in a dry conversion of UF_6 to UO_2.(Integrated Dry Route, IDR process). This process does not involve nitrogen compounds.

Besides the powder fabrication process (ADU or AUC), several additives possibly included during the fuel pellet fabrication as well as some specific pellet sintering atmospheres (like cracked ammonia) may also be responsible for the introduction of nitrogen in the fuel.

Nitrogen contained in the as-fabricated fuel is reported to be present as uranium nitrides [12].

As regards the as-fabricated cladding, nitrogen is expected to be in solid solution, taking into account its solubility properties [13].

For what concerns the chemical form of ^{14}C in the irradiated fuel, [7] suggested carbide, oxycarbide and elemental carbon as possible forms, but with no experimental confirmation.

Studies performed by [16], indicated that at least a significant part of the carbon contained in the fuel must be in the elemental form as its chemical activity does not depend on its concentration and therefore, it must not be in solution in the UO_2.

In the fuel rod cladding, ^{14}C produced from nitrogen during irradiation can be considered as quasi-stationary [17,18,19]. It may diffuse slowly to segregated carbides.

During irradiation, either nitrogen precursor or ^{14}C itself are liable to migrate inside the fuel pellet, towards UO_2 grain boundaries as well as to the fuel-cladding gap and thus contribute to the radionuclides instant release at the time the stored fuel rod integrity will be lost.

As irradiation proceeds, fission products are generated and oxygen atoms are freed. According to [14], the oxygen liberated in the irradiated fuel might be redistributed by gas phase thermomigration of CO/CO_2 , through cracks and open porosity, using the C impurity as well as the produced ^{14}C.

On the other hand, [12,15] has reported that the presence of excess oxygen will produce irreversible release of nitrogen precursor from the fuel.

However, as concerns LWR fuels, the fuel global stoichiometry is in fact only slightly modified during irradiation, as oxygen consuming elements are present in the fuel rod, with essentially:

- The zirconium of the cladding, which oxidises at the inner surface,
- Molybdenum fission product, with a significant fission yield, and with a Mo/MoO_2 thermodynamic equilibrium reached at an oxygen potential very close to that prevailing in the fuel operation conditions during irradiation. Mo will thus buffer the oxygen potential.

The two migration processes mentioned above are not expected to lead to major ^{14}C accumulation in the fuel rod open volumes.

In the analyses reported by [3] and [10], the fraction of ^{14}C contained in the filling gas of the fuel rod (compared to the total content measured on the fuel rod) is lower than 0.1 %.

One expects that ^{14}C eventually precipitated at the inner surface of the fuel cladding after migration would be in the form of zirconium carbide or zirconium cyanonitride [20], and will be present near the surface only, because of the slow diffusion properties of nitrogen and carbon in zircaloy [18,19].

A large number of leaching experiments have been performed on irradiated fuel samples, in order to assess the contribution of ^{14}C to radionuclides instant release (amongst them, one notes for example [21] and [22], performed on PWR fuel and [23], performed on CANDU fuel).

This contribution is conservatively assumed to be larger than the one of the ^{14}C contained in the fuel rod open volumes (including only the fuel open porosity and cracks, besides the fuel-cladding gap) and to concerns in addition all the grain boundary inventory.

According to the results of the above-mentioned leaching experiments on unclad crushed fuel, one may assume that the maximum contribution of ^{14}C, relatively to its total production in the fuel, will remain below 10 %, for standard-operated LWR fuel.

Conclusions

On the basis of calculation and experiment results on PWR fuel and of their comparison, one can state that the use of the ASTM specification for nitrogen content in UO_2 pellet as input for the ^{14}C source term evaluation is reasonably conservative.

Negligible gaseous ^{14}C is present in the rod filling gas.

Most of the ^{14}C produced in the fuel rod remains in the fuel matrix and in the zircaloy cladding and will not participate to the radionuclides instant release.

Base on extended experimental results, a maximum of 10´ % of the ^{14}C produced in the fuel will be included in the radionuclides fast release occurring when spent fuel comes in contact with groundwater.

References

[1] BELGONUCLEAIRE, in plant measurements for quality control. FBFC, in plant measurements for quality control.

[2] de Wouters R., Characterisation of Irradiated Fuel Assemblies : Radionuclide Inventory in Spent Fuel Elements. BELGATOM report 0204246/221, June 2003.

[3] Bleier A., Neeb K.H., Kroebel R.H., Wiese H.W., Carbon-14 Inventories and behaviour in LWR-Spent Fuel Rods During Reprocessing. RECOD 87, Nuclear Fuel Reprocessing and Waste Management.

[4] Croff A.G., Alexander C.W., Oak Ridge National Laboratory Report ORNL/TM-7431. Oak Ridge, TN, 1980.

[5] Murphy B.D., Characteristics of Spent Fuel from Plutonium Disposition Reactors. Vol. 3: A Westinghouse Pressurized-Water Reactor Design. Oak Ridge National Laboratory Report ORNL/TM-13170/V3. Oak Ridge, TN, 1997.

[6] Baudoin P., Gay D., Certes C., Serres C., Alonso J., Lührmann L., Martens K-H., Dodd D., Marivoet J., T. Vieno, Spent Fuel Disposal Performance Assessment: the SPA Project. European Commission Report EUR 19132 EN, 2000.

[7] Van Konynenburg R.A., Smith C.F., Culham H.W., Smith D.H., Carbon-14 in Waste Packages for Spent Fuel in a Tuff Repository. Material Research Society Symposium Proceeding Vol. 84, 1987.

[8] Campbell D.O., Light Water Reactor Nuclear Fuel Cycle. Edited by Wymer R.G., Vondra B.L., Jr. CRC Press, Inc., Boca Raton, FL, 1981.

[9] Stone J.A., Johnson D.R., Proceedings of the 15th D.O.E. Nuclear Air Cleaning Conference. Boston, MA, August 7-10,1978.

[10] Barner J.O., Pacific Northwest Laboratory Report PNL-5109 Rev.1. Richland, WA, 1985.

[11] Wilson C.N., Hanford Engineering Development Laboratory Report HEDL-TME 85-22 Richland, WA, 1986.

[12] Ferrari H. M., Report WCAP 2098, Westinghouse Atomic Power Division, Pittsburg, PA, 1961.

[13] Hansen M., Anderko K., Constitution of Binary Alloys. McGraw-Hill, New-York, 1958.

[14] Rand M.H., Roberts L.E.J, Thermodynamics, Proceedings of the Symposium on Thermodynamics with Emphasis on Nuclear Materials and Atomic Transport in Solids. Vienna, July 22-27, 1965.

[15] Ferrari H.M., Nuclear Science and Engineering 17, 503. 1963.

[16] Adamson M.G., Journal of Nuclear Materials 38, 213, 1971.

[17] Agarwala R.P., Paul A.R., Journal of Nuclear Materials 58, 25, 1975.

[18] Perkins R.A., Carlson P.T., Met. Trans. 5, 1511, 1974.

[19] Anttila A., Räisänen J., Keinonen J., Journal of Less-Common Metals 96, 257, 1984.

[20] Blumenthal W.B., The Chemical behavior of Zirconium. Van Nostrand, Princetown,N.J., 1958.

[21] Neal W.L., Rawson S.A., Murphy W.M., Mat. Res. Soc. Symp. Proc. 112, 505, 1988.

[22] Wilson C.N., Pacific Northwest Laboratory Reports PNL-7169 and 7171. Richland, WA, 1990.

[23] Stroes-Gascoyne S., Tait J.C., Porth R.J., McConnell J.L., Lincoln W.J., Release of ^{14}C from the gap and grain boundary regions of used CANDU fuels to aqueous solutions. Waste Management Vol.14, N°5, 385, 1994.

Migration of C-14 in Activated Metal under Anaerobic Alkaline Condition

N. Kogawa, NDC

Introduction

The activated metal which has been used in the nuclear power plant will be disposed in a geological repository. For the safety assessment of radionuclide migration, it is necessary to access not excessively conservatively but actually. C-14 is considered an important nuclide for the safety assessment of geological repository facility. However there has been little observation data on the leaching rate of C-14 in activated metal.

It was the aim of this investigation to provide data relevant to design the model of C-14 migration mechanism, by dual determinations of leaching rate and corrosion rate.

Corrosion Test

Experiment

The metals of specimens were the same metals as the metals of specimens for C-14 Leaching test (See below for further details) but weren't activated metals, zirconium alloy, stainless steel, and nickel alloy. All the metals were cut into the shape of plate as flag and polished. The corrosion test had been performed under anaerobic alkaline condition simulated in the disposal environment (show Tab.1).

Tab. 1: Condition of Corrosion Test

Material of Specimen	- Zirconium Alloy - Stainless Steel - Nickel Alloy
Sharp of Specimen	- Plate as Flag (Show Fig. 1)
Surface on Specimen	- Elimination of Oxide-Film by Polishing
Environment of Test	- Anaerobic Alkaline Condition
Method of Measurement	- Polarization Resistance Measurement & Best-fit Curve Calculation

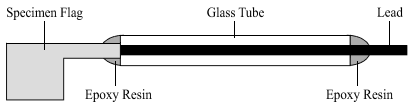

Fig. 1: Schematic Diagram of Specimen for Corrosion Test

The experimental setup used is illustrated in Fig. 2. A polarization resistance measurement was applied to measure the corrosion current (corrosion rate). The corrosion current has been computed using the best-fit curve calculation of Mansfeeld. The polarization resistance measurement is possible to measure the small corrosion current over a long period of time. And the best-fit curve calculation is possible to obtain the corrosion parameters by graphical analysis of polarization curve.

In the measurement, two test material electrodes have been applied; one is as a reference and the other is as a working electrode. It is possible to keep the experiment condition for long time easy by using a simple experimental setup.

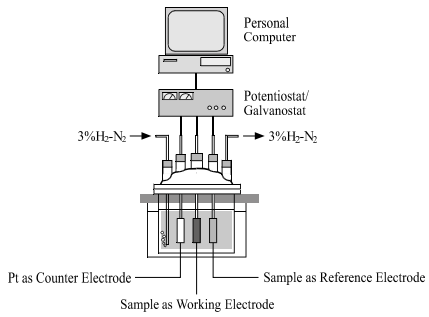

Fig. 2: Schematic Diagram of Test Equipment for Polarization Resistance Measurement

Fig. 3 shows corroded depth of silver alloy, one is calculated with corrosion current by the polarization resistance measurement, and the other is calculated with corrosion product by the chemical analysis. As shown in Fig. 3, these two data are in good agreement.

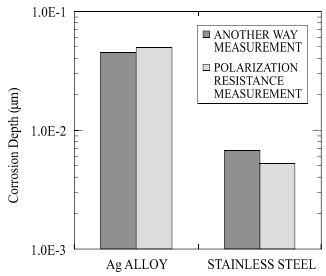

Fig. 3: Comparison between Polarization Resistance Measurement and Alternate Measurements

Corrosion depth is calculated with result by polarization resistance measurement, chemical analysis (Silver Alloy) and radio chemical analysis (stainless steel).

Result

The results of corrosion rate plotted as function of time are shown in Fig. 4. The graph shows that the corrosion rate decreases abruptly after steeping and then become stable at small rate, and trend as following.

zirconium alloy < nickel alloy < stainless steel

After the test, corrosion products aren't observed on the surface of specimens. In order to evaluate the behavior of oxidation, X-ray photoelectron spectroscopy (XPS) was performed to the surfaces of specimens. The results of XPS show that chromium is concentrated in the corrosion product on the stainless steel and nickel alloy.

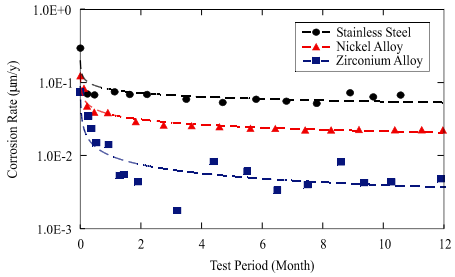

Fig. 4: Corrosion Rate of Zirconium Alloy, Stainless steels and Nickel Alloy as a Function of Time after Steeping

Discussion

The trend of corrosion currents of some metals in Fig.5 can be explained in qualitative by properties of material and one's corrosion products.

1. When stainless steel and nickel alloy are steeped into the anaerobic alkaline water, a corrosion product consisted mainly of chromium hydroxide forms on the surface. The corrosion is inhibited because one has corrosion resistance and therefore the corrosion current decreases. Further more the nickel being nobler than iron, is the main component of stainless steel. The corrosion currents are therefore smaller than that of stainless steel.
2. Because a zirconium is too reactive with water, a zirconium alloy is corroded and a corrosion product forms on the surface concomitantly with steeping. The corrosion current is quite small because zirconium oxide is a stable nonconductor therefore this has a good corrosion resistance.

C-14 Leaching Test

Experiment

Three kinds of metals; activated zirconium alloy, activated stainless steel, and activated nickel alloy were used for the test specimens in this work, which had been used at nuclear power plant. The activated zirconium alloy specimens were prepared by a similar method to the treatment method of spent fuel in a reprocessing plant and cut into short length tube. The activated stainless steel specimens and the nickel alloy specimens were cut into plate. All the specimens were eliminated the oxide film by polishing. The leaching test had been performed under anaerobic alkaline condition simulated the disposal environment (show Table 2).

Tab. 2: Condition of C-14 Leaching Test

Material of Specimen	- Activated Zirconium Alloy - Activated Stainless Steel - Activated Nickel Alloy
Shape of Specimen	- Zirconium Alloy Tube - Stainless Steel / Nickel Alloy Plate
Surface on Specimen	- Elimination of Oxide-Film by Polishing
Environment of Test	- Anaerobic Alkaline Condition

The specimen was immersed in the test solution of simulated groundwater for a certain period. And then a quantity of C-14 in the test solution was analyzed. In this method of analysis, inorganic carbon in the test solution is brought into contact with inorganic acid to form carbon dioxide and discharged for a measurement as inorganic carbon. Next, an oxidizing agent is added to the remaining test solution to oxidize and discharge all carbon as carbon dioxide for its measurement as organic carbon.

Result

Table 3 shows the results of leaching test. Most of the C-14 released from radioactive metal and existing in the leached liquid was in organic form.

Tab. 3: Results of Leaching Test

Activated Zirconium Alloy			**Bq/Unit**
Test Period (Month)	5.5	9	11.5
-	1.1×10^{1}	1.5×10^{1}	1.6×10^{1}

Activated Stainless Steel			**Bq/Unit**
Test Period (Month)	1	3	6
High Irradiated	8.7×10^{-1}	7.9×10^{-1}	1.9×10^{0}
Low Irradiated	4.3×10^{-1}	2.0×10^{0}	ND

Activated Nickel Alloy				**Bq/Unit**
Test Period (Month)	1	3	6	11
High Irradiated	ND	ND	ND	2.9×10^{-1}

Discussion

The comparison of the C-14 leaching rate between the C-14 leaching test results data and calculated value from corrosion test results is shown in Fig.5. The graph indicates as following.

1. The C-14 leaching test results coincide approximately with the leaching rate calculated from corrosion rates.
2. The C-14 leaching rate of high irradiated stainless steel is lower than the one of low irradiated stainless steel. The formation of oxide file steel has been observed on the high irradiated stainless immediately after being polish. Therefore, the lower leaching rate is due to the oxide film which functions as passive film and then reduces the amount of corrosion.

Conclusion and Future

The C-14 leaching test and the corrosion test have been carried out to design the model of C-14 migration mechanism. The main results obtained are shown below.

- The C-14 leaching test results coincide approximately with the leaching rate calculated from corrosion rates.

Our plans for the near future are:

- The estimation about the influence of fluctuation in disposal environment parameters for C-14 migration behavior.

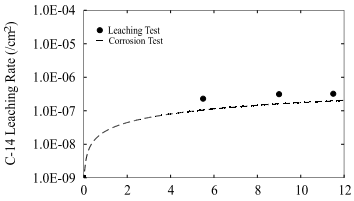

(a) Zirconium Alloy

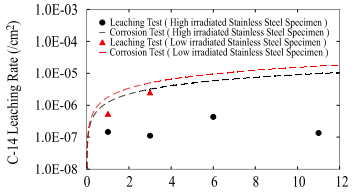

(b) Stainless Steel

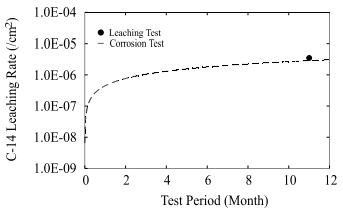

(c) Nickel Alloy

Fig. 5: Comparison of C-14 Leaching Rate between Results of C-14 Leaching Test and calculated value from Corrosion Test Results

Circle / Triangle: Results of C-14 Leaching Test
Broken Line: Leaching Rate calculated from Results of Corrosion Test

Modelling the Partitioning and Transport of C-14 in a Microbially Active LLW Site

J. Small
BNFL Nuclear Sciences and Technology Services, H460, Hinton House,
Risley Warrington WA3 6AS UK.
(joe.s.small@bnfl.com)

Introduction

The Drigg site is an operational facility for the near-surface disposal of solid low level radioactive waste (LLW) in the UK. The site is located in north-west England and is owned and operated by British Nuclear Fuels plc (BNFL). Disposals are carried out under the terms of an authorisation granted by the UK Environment Agency. The authorisation is periodically subject to formal regulatory review and in September 2002 BNFL submitted a Post Closure Safety Case (PCSC) (BNFL, 2002a) to the Environment Agency. The PCSC was supported by a Post Closure Radiological Safety Assessment (PCRSA) (BNFL, 2002 b,c,d,e) which considered the radiological pathways through groundwater, gas and through future human actions and disruptive events.

The Drigg site includes two disposal systems (Fig. 1) An original system operated from 1959 to 1988 comprising a series of parallel trenches excavated into glacial clays, back filled with LLW and covered with an interim water resistant cap. 2) Current disposal of compacted waste placed in steel ISO-freight containers, with void space filled with a highly fluid cement based grout. These containers are then disposed of in a series of open concrete vaults. The Drigg radionuclide inventory considered by the PCRSA (BNFL 2002f) comprises a total of 13.1 TBq of C-14 of which 0.35 TBq was disposed in the trenches and the remainder comprising current and future LLW arisings disposed in the cementitious vault. The form of C-14 in the LLW inventory is not well characterised and comprises a variety of waste streams in the UK national inventory (Electrowatt-Ekono, 1999). The majority of C-14 is likely to be present as activation products in steel, concrete and graphite.

Drigg LLW contains a significant proportion of organic cellulose based waste together with waste steel and other metals. Other reactive materials comprising the vault wasteform include cementitious materials used to fill voidage and the steel ISO-freight containers. These reactive components of the LLW and the wasteform may all affect chemical reactions involving carbon through a variety of biogeochemical processes and interactions, which include microbial processes. The release and transport of C-14 present in Drigg LLW will depend on the processes of waste degradation that involve the very much larger amounts of stable carbon (C-12, C-13) present in the repository.

In order to understand the complex interactions of processes involved in the Drigg near-field BNFL have developed a mechanistic model which considers feature, events and processes (FEPs) that may affect the release and transport of chemically reactive radionuclides. This model includes specific routines to consider the partitioning of C-14 which aim to provide a realistic source term of C-14 release in groundwater and gas. The objectives of this paper are to present an overview of the modelling approach and some example results of the Drigg 2002 PCRSA source term calculations. In addition a discussion and further calculations are presented to evaluate the significance of the effects of isotopic fractionation which was identified by the

initial FEPs screening process forming part of the systematic approach used in the PCRSA methodology.

The DRINK Source Term Model

The DRINK (DRIgg Near-field Kinetic) model utilises the BNFL biogeochemical reaction Generalised Repository Model (GRM) (Manton *et al*, 1995; Humphreys *et al*, 1995; Small *et al*, 2000, 2003) to simulate the evolving geochemistry of the Drigg trenches and vaults. GRM considers kinetically controlled steel corrosion and microbial induced cellulose degradation processes. The reaction products formed during the processes are used to determine an evolving redox condition, taking account of kinetically controlled microbially mediated redox reactions between product species and species in groundwater (e.g. SO_4), and minerals in soils (e.g. $Fe(OH)_3$). Redox potential (pe) is calculated by using standard mass action equations (Stumm and Morgan, 1981) considering the most oxidising couple. The resulting pe is used as a constraint for equilibrium speciation and mineral equilibrium calculations by a routine based on PHREEQE (Parkhurst *et al*, 1980), which determines the pH and master species concentrations, including those radionuclides which are solubility controlled. GRM describes the 2-dimensional lateral groundwater flow in the saturated zone by means of a finite difference solver. The discretisation of the finite difference grid used in the DRINK model is shown in Fig. 1. Vertical flow is considered on a cell by cell basis and is used to simulate the release of radionuclides from the unsaturated zone to the saturated zone. In DRINK, sorption is modelled using a distribution coefficient (Kd) which is selected taking into consideration the simulated geochemical model, and the types of sorbant surfaces present in the Drigg trenches and vaults. Radioactive decay is considered on a cell basis for dissolved, sorbed and precipitated phases, and for the unsaturated zone.

Modelling the partitioning of C-14

Specific routines are included in the GRM code which follow C-14 through the various microbial and chemical speciation reactions that involve carbon. The C-14 inventory can be initially assigned to materials which release C-14 either as a kinetic function (e.g associated with hydrolysis of cellulose), or as a fraction of a solubility controlled mineral phase (e.g $CaCO_3$). Because the chemical nature of C-14 in the Drigg inventory is not well constrained it is assumed for the main simulation of the PCRSA that C-14 is present in the most reactive phase, cellulose. This approach is conservative with respect to the groundwater and gas radiological pathways.

C-14 is followed through the model as a fraction of moles of C-14 present in a chemical species to the total moles of carbon present in the species. For each model calculation cell, at each timestep, the fraction of C-14 in product species of a chemical speciation reaction or microbial process is recalculated assuming that the product species has a homogeneous carbon isotope composition. In this way C-14 released from cellulose is redistributed amongst product aqueous, gaseous and solid phases and this provides a source term of C-14 for assessment calculations.

Chemical Results of the DRINK Model

The DRINK model outputs concentrations of chemical species and microbial products, which support the conceptual understanding of the interaction of FEPs relevant to the PCRSA. Some example output is presented in Figures 2 to 5 where the concentrations are plotted for each DRINK model cell representing the trenches and vaults (Fig. 1). Variation in the parameters between cells reflects the heterogeneity of the Drigg trenches and vaults inventory as well as

effects of cell location and influence of boundary groundwater condition. In the case of the Drigg trenches the model simulates that acidic and reducing conditions are developed for a period of several thousand years (Figures 2 and 3). This is consistent with characterisation of the chemical conditions within the trenches and with experimental studies of waste degradation (BNFL, 2002g). Acidic and reducing conditions result from the organic degradation and corrosion processes that occur. Eventually, after waste degradation processes slow, pH and redox potential (pe) return to that of the local groundwater. In the case of pH the hysteresis that occurs, where elevated pH rises above that of groundwater is a consequence of continuing corrosion processes which generate alkalinity. At earlier times organic degradation processes which generate acidity through CO_2 and organic acidic predominate. Fig. 4 illustrates the concentration of acetate that develops associated with organic degradation, acetate is of course notable since it represents a potential transport vector for C-14.

In the Drigg vaults the chemical conditions are additionally influenced by the presence of cementitious materials which buffer the pH to around pH 10-11. As a consequence of the alkaline conditions developed and the CO_2 generated from degradation of organic materials and input from groundwater calcium carbonate precipitation occurs (Fig. 5). Carbonate precipitation has the potential to immobilise C-14 under the simulated vault chemical conditions.

C-14 Partitioning and Release from the Drigg near-field

Example output of C-14 data from DRINK calculation cells representing the Drigg trenches are presented in Figures 6 to 8. Aqueous C-14 (Fig. 6) comprises the concentration of C-14 present in aqueous carbonate species and acetate species. Gaseous C-14 (Fig. 7) comprises the moles of CO_2 and CH_4 present in a gas headspace associated with each DRINK cell. Solid C-14 (Fig. 8) is present in the form of the original source cellulose, within microbial biomass and in secondary carbonate minerals. Fluctuations in the aqueous and gaseous C-14 occur as a result of the effects of the various chemical and microbiological processes. Peak aqueous concentrations of aqueous C-14 occur during the first 1,000 years during which time organic degradation is active. An increase in C-14 in the gaseous phase occurs after this period of degradation which are related to redoxidation processes that release C-14 immobilised in iron carbonate corrosion product. The effects of radioactive decay are evident in all three phases by the decline in C-14 after 5,000 years.

Fig. 9 and Fig. 10 illustrate how the C-14 inventory present in individual cells located in the trenches and vaults is partitioned between mobile and immobile phases during the model simulation. In the case of the trenches (Fig. 9) the majority of the C-14 inventory is released from the cell by transport in the aqueous phase (*curve C-14 released*). Around 10 % of the C-14 is immobilised in biomass representing recycled organic material, only a small proportion, around 1 %, is immobilised in the form of secondary carbonate solid phases.

In contrast, in the case of the vaults (Fig. 10) C-14 is immobilised in the form of secondary carbonates formed under the alkaline conditions of the cementitious grouted waste. In this case around half of the C-14 inventory is released in groundwater from the model cell and the remainder is immobilised.

Carbon Isotope Fractionation

The fractionation of C-14 with the more abundant stable isotopes of carbon has the potential to enrich both mobile and immobile phases in C-14 as a result of the preferential uptake of the different carbon isotopes. As a result isotope fractionation could affect the source term of C-14. Isotope fractionation of the minor isotopes of carbon (C-14 and C-13) occurs during chemical reactions and phase changes as a consequence of slight differences in the strength of chemical bonds involving different isotopic species. Molecules containing heavy isotopes have a higher dissociation energy and are hence more stable than those with lighter isotopes. Examination of the stable isotope distributions in gases, fluids, mineral and organic matter provides an invaluable tool in understanding and quantifying biogeochemical reaction processes (O'Neill, 1986; Grossman, 1997; Plummer *et al*., 1994; Kendall and Caldwell, 1998; Zyakun, 1995, 1996). Isotopic fractionation can be described as either an equilibrium or kinetic process (O'Neill, 1986). Liquid vapour fractionation of oxygen and hydrogen in water is normally referred to as an equilibrium process, where forward and backward rates of exchange are equal. Mineral dissolution and precipitation are also often considered to result in equilibrium isotope exchange. Many biological processes result in kinetic isotope fractionation where organisms preferentially utilise lighter isotopes because of the lower energy required to break chemical bonds (Grossman, 1997). As a consequence lighter isotopes are used preferentially at a faster rate. Consequently, biologically mediated products are enriched in lighter isotopes. The extent of isotopic fractionation between two phases A and B is given by the fractionation factor (α) where:

$$\alpha_{A-B} = \frac{^{13}C_A / ^{12}C_A}{^{13}C_B / ^{12}C_B}$$

The fractionation of C-14 can be assumed to be analogous to C-13/C-12 fractionation which has been studied widely. C-14 is much less abundant in nature than the stable isotope C-13 and C-14/C-12 fractionation is not generally used in the study of natural biogeochemical processes. C-14 is however used extensively for radiometric dating and in this context the fractionation of C-14 must be quantified to apply a correction to C-14 age dates. The standard practice in C-14 radiometric dating when estimating fractionation is to assume that the fractionation factor (α) for C-14/C-12 fractionation is twice that of C-13/C-12 fractionation (Plummer *et al*.,1994), although there is evidence that fractionation of C-14/C-12 may be up to 2.3 times that of C-13/C-12 (Plummer *et al*., 1994). Many reviews of C-13/C-12 fractionation between groundwaters, minerals, organics and biota are available from which appropriate C-14/C-12 fractionation factors can be estimated. Grossman (1997) provides a particularly useful review of processes influencing C-13/C-12 fractionation considering both inorganic and microbiological fractionation.

Modelling the effect of C-14/C-12 fractionation

The extent to which C-14 may be enriched in mineral and aqueous carbonates can be quantified by considering the mass transfer of carbon containing species and phases simulated by the DRINK model. DRINK provides summary output for each mineral, aqueous and organic (microbial substrate/product) phase as a total mass in the DRINK model at each output time step. This output data can be used to calculate (in a simplified manner for the whole site inventory) the number of moles of carbon in each phase and hence the mass transfer of carbon can be followed. Using this DRINK output, it has been possible to incorporate the effect of

isotopic fractionation by redistributing the mass of C-14 released during reaction between groups of species according to the fractionation factor (α).

The C-14 fractionation model thus requires input values of the fractionation factor between the phases considered and a reference phase (CO_2 gas). Tab. 1 lists the list of phases (species) and values of α used in the calculation which were selected on the basis of a review of literature on fractionation of C-13. The fractionation factors in Tab. 1 were chosen to consider maximum levels of C-14/C-12 fractionation and represent around twice that of the maximum fractionation observed for C-13.

Tab. 1: C-14/C-12 Fractionation factors

Phase	*Fractionation Factor (α)*
CO_2 gas (reference)	1.0
Dissolved Carbonate	1.1
Acetate	0.8
Microbial Biomass	0.9
Carbonate Minerals	1.2

Fig. 11 compares the results of the DRINK model output which excludes the effects of isotope fractionation with the alternative calculation where effects of isotope fractionation were examined. The comparison indicates that the effect of fractionation is small. The C-14 content of the various mobile and immobile phases is affected by only a small degree which is of less significance than that resulting from other uncertainties, such as the chemical form of C-14 in the LLW inventory. By including the effects of fractionation the C-14 content of the immobile mineral (carbonate) phase, which is the dominant C-14 containing phase for the whole site, is enriched. Thus in terms of the groundwater and gas radiological pathways it is conservative to ignore the effects of isotopic fractionation.

Summary and Conclusions

A mechanistic model of the biogeochemical processes associated with the degradation and interaction of LLW with groundwater in a surface disposal setting has been developed. This model has been used to provide a cautious realistic assessment of the release and transport of C-14 from the near-field taking account of the complex series of chemical and microbial processes that involve carbon. The model provides a time varying source term of C-14 in the aqueous, gaseous and solid phases that has been used in performance assessment calculations.

The model indicates that C-14 is immobilised by the incorporation into $CaCO_3$ formed in the Drigg cementitious vault disposal system which is used currently, and is planned to be used for future disposals. Overall around 80 % of the C-14 assigned to the vaults is immobilised. For the older Drigg trench disposal system, which contains a smaller inventory of C-14 the model indicates that C-14 is not retained and is released mainly through groundwater over a period of several thousand years.

The effect of isotope fractionation in affecting the redistribution of C-14 and hence the C-14 source term has been investigated by a review of literature on C-13/C-12 systematics and by some additional model calculations. This has shown that the effect of fractionation is small compared to other uncertainties and that it is the immobile carbonate phase that becomes enriched in C-14.

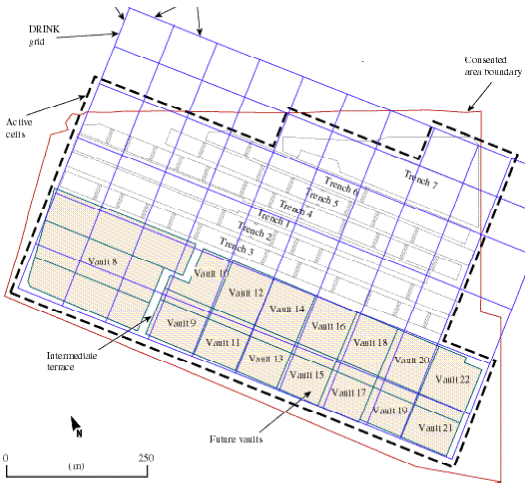

Fig. 1: Layout of the Drigg trenches and vaults, overlain by the DRINK grid (BNFL, 2002g)

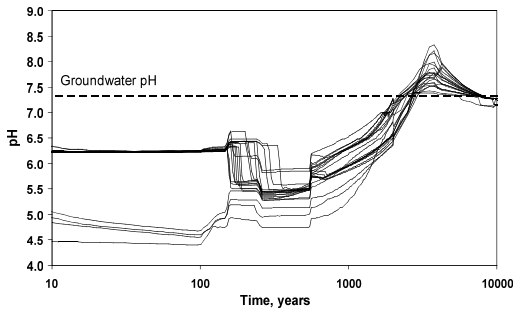

Fig. 2: Variation in pH for the Drigg trench DRINK model cells

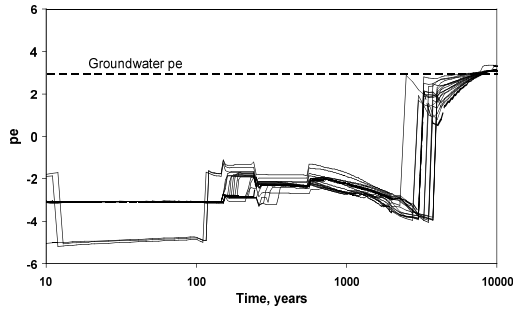

Fig. 3: Variation in redox potential (pe) for the Drigg trench DRINK model cells

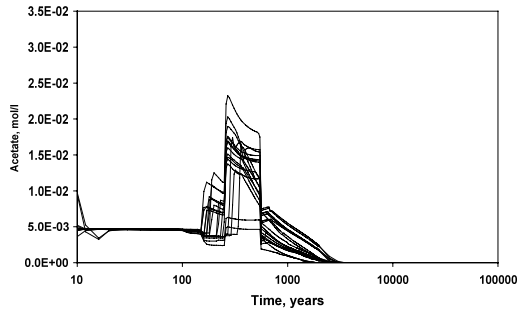

Fig. 4: Variation in acetate concentration for the Drigg trench DRINK model cells

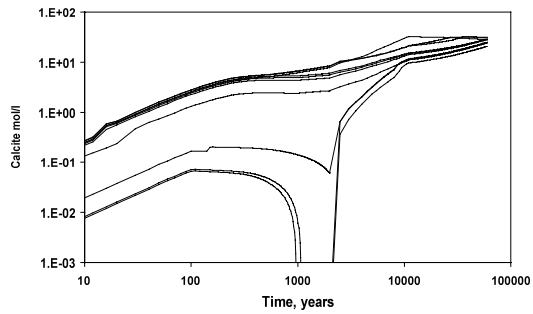

Fig. 5: Variation in calcite ($CaCO_3$ precipitate) concentration for the Drigg vault DRINK model cells

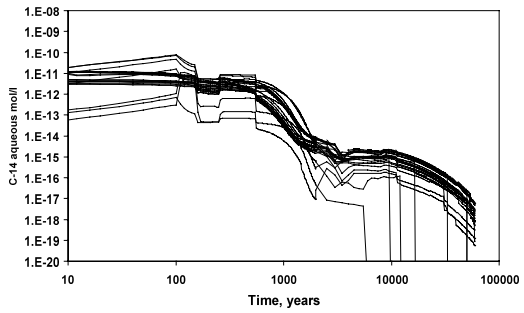

Fig. 6: Variation in C-14 present as aqueous species for the Drigg trench DRINK model cells

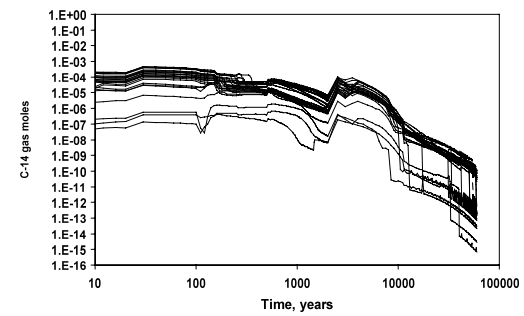

Fig. 7: Variation in C-14 present as gaseous species for the Drigg trench DRINK model cells

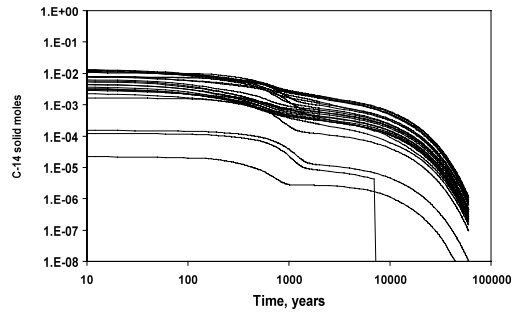

Fig. 8: Variation in C-14 present as solid phases for the Drigg trench DRINK model cells

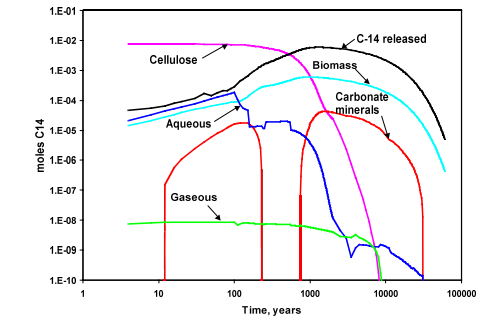

Fig. 9: Redistribution of C-14 from the initial form in cellulose to product mobile and immobile phases for an example DRINK model cell for the trenches

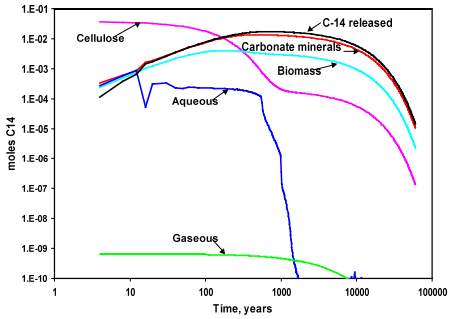

Fig. 10: Redistribution of C-14 from the initial form in cellulose to product mobile and immobile phases for an example DRINK model cell for the trenches

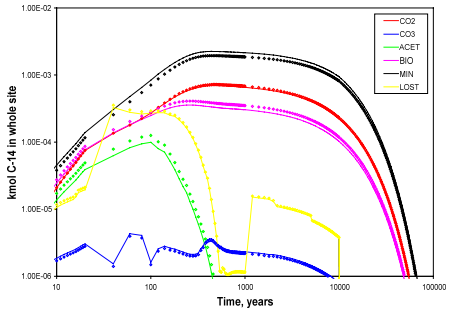

Fig. 11: Comparison of the calculated ^{14}C content of the carbon containing phase for the case with no isotope fractionation (symbols) with that for the maximum likely levels of fractionation (lines)

References

BNFL, 2002a. Drigg Post-Closure Safety Case: Overview report.

BNFL, 2002b. Drigg Post-Closure Safety Case: PCRSA Approach.

BNFL, 2002c. Drigg Post-Closure Safety Case: PCRSA Scenarios and Calculation Cases.

BNFL, 2002d. Drigg Post-Closure Safety Case: PCRSA Process System Analysis.

BNFL, 2002e. Drigg Post-Closure Safety Case: PCRSA Results.

BNFL, 2002f. Drigg Post-Closure Safety Case: Inventory of Past and Potential Future Disposals.

BNFL, 2002g. Drigg Post-Closure Safety Case: Near-Field Biogeochemistry.

Electrowatt-Ekono, 1999. The 1998 United Kingdom radioactive waste inventory. DETR/RAS/99.009, Nirex Report N3/99/01 (and associated reports DETR/RAS/99.003 - 008, N3/99/02 - 07).

Grossman, E.L., 1997. Stable Carbon Isotopes as Indicators of Microbial Activity in Aquifers. In: *Manual of Environmental Microbiology*, Hurst, C.J., Knudsen, G.R., McInerney, M.J., Stetzenbach, L.D. and Walter, M.V. American Society For Microbiology. p565-576.

Humphreys, P. N., Johnstone, T., Trivedi, D. and Hoffmann, A., 1995. in *Scientific Basis for Nuclear Waste Management XVIII*, edited by T. Murakami and R.C Ewing. Mat. Res. Soc. Proc., **353**, 211-218.

Kendall, C, and Caldwell, E.A., 1998. Fundamentals of Isotope Geochemistry. In: *Isotope Tracers in Catchment Hydrology* Eds C.Kendall and J.J.McDonnell. Elsevier Science B.V, Amsterdam. p51-86.

Manton, S., Johnstone, T., Trivedi, D. P., Hoffmann, A. and Humphreys, P. N., 1995. Radiochimica Acta, **68**, 75-79.

O'Neil, J.R., 1986. Theoretical and experimental aspects of isotopic fractionation. In: *Stable Isotopes*, (Ed. J.W. Valley, H.P. Taylor and J.R. O'Neil), Mineralogical Society of America, *Reviews in Mineralogy*, **16,** p1-40.

Parkhurst, D.L., Thorsteson, D.C. and Plummer, L.N., 1980. PHREEQE – A computer program for geochemical calculations, USGS Water Resour. Invest., 80-96.

Plummer, L.N., Prestemon, E.C. and Parkhurst, D.L., 1994. An interactive code (NETPATH) for modeling NET geochemical reactions along a flow PATH, Version 2.0. *United States Geological Survey Water-Resources Investigations Report 94-4169*.

Small. J.S., Humphreys, P.N., Johnstone, T.L. Plant, R. Randall, M.G. and Trivedi, D.P., 2000. Results of an aqueous source term model for a radiological risk assessment of the Drigg LLW site, UK. *Scientific Basis for Nuclear Waste Management XXII*, Materials Research Society.

Small. J.S., 2003. A comparison of site characterisation data and modelling results from a radiological assessment of the Drigg low level radioactive waste disposal site. *Materials Research Society Symposium, Scientific Basis for Nuclear Waste Management XXVII, Kalmar Sweden, June 2003.* (In press).

Stumm, W. and Morgan, J.J., 1981. *Aquatic Chemistry*. 2nd Ed.. Wiley, New York, p449.

Zyakun, A.M., 1995. Stable carbon isotope discrimination by heterotrophic microorganisms (review) *Applied Biochemistry and Microbiology*, **32**, p153-159.

Zyakun, A.M., Bondar, V.A., Namsearaev, B.B., 1996. Fractionation of methane carbon isotopes by methane oxidizing bacteria. *Freib. Forsch*., **360** p19-27.

Application of a new gas generation model to develop the source-term of Carbon-14 bearing gases in radioactive waste disposal

S. Vines, S. Norris and A. Harris
United Kingdom Nirex Limited

Introduction

Nirex is the UK waste management organisation, aiming to provide the UK with safe, environmentally sound and publicly acceptable options for the long-term management of radioactive materials. One such option is phased deep geological disposal of intermediate level waste and some low-level waste. The Nirex phased disposal concept [1] envisages:

- immobilisation and packaging of wastes
- interim surface storage
- transport to a repository
- emplacement in vaults excavated deep underground within a suitable geological environment
- a period of monitoring, during which the wastes would continue to be retrievable in a relatively straightforward manner
- backfilling of the repository at a time determined by future generations
- sealing and closure of the repository.

C-14 is a key radionuclide in the management of radioactive waste, because it has the potential to be released as a gas. Nirex undertakes assessments of gas generation from packaged wastes in the UK radioactive waste inventory for the following purposes:

- Providing packaging advice to waste producers
- Modelling the operational period of a repository
- Modelling the post-closure period of such a repository.

Past and current assessments of the groundwater and human intrusion pathways have considered the C-14 content of all wastes as declared in the inventory [2]. Assessments of the gas pathway, however, have been limited to the risks associated with the generation of carbon-14 bearing gases from degradation of carbon-14 labelled organic wastes. This paper summarises the radiological consequences from C-14 in current gas assessments and goes on to describe recent work to identify additional sources of C-14 in UK waste and to include the potential release of C-14 containing gases from such wastes in a simplified model of gas generation.

Radiological consequences

In the current Nirex assessment of the gas pathway, using the software GAMMON, only risks associated with the generation of carbon-14 bearing gases from degradation of carbon-14 labelled organic wastes are considered. Carbon-14 can be present as a gas in the form of carbon dioxide or methane. In the current Nirex reference case model it is assumed that all the carbon-14 bearing carbon dioxide reacts with cementitious grout inside the waste containers or with the cement-based backfill; the radiological hazard arising from this gas is therefore assessed as insignificant. This approach is consistent with that taken in previous Nirex work (e.g. Nirex 97 [3]).

In the post-closure performance assessment, releases are calculated for two scenarios: release to the interior of buildings and release to the outdoor environment. The calculated radiological risk from carbon-14 bearing methane is influenced by assumptions made about the consumption of carbon-14 bearing methane by microbes in soil, as this ultimately affects uptake of carbon-14 in the food chain by humans. (The main potential radiological hazard from the release of carbon-14 in methane to the surface arises from the ingestion route, with plant uptake of the active gases; risks from inhalation within buildings are significantly smaller than those from discharge to the soil.)

Tolerable generation rates of repository-derived carbon-14 bearing methane in the post closure phase, which are consistent with the UK regulatory risk target of 10^{-6}/yr, can be calculated on the assumption of direct discharge to a specified surface area. (The gas travel time from the repository to the surface is assumed to be insignificant compared with the half-life of carbon-14.) Tolerable generation rates are listed in Table 1, calculated on the basis of release to an area of 10,000 m^2. This area is smaller than the plan area of the repository in the phased disposal concept, implying gas flow focussing has occurred.

Tab. 1: Tolerable carbon-14 bearing methane generation rates in the post closure phase

Gas	Tolerable rate of gas generation (TBq/year)	
	Release to the interior of buildings	Release to the outdoor environment
14-CH_4	8.13	2.38 10^{-5}

As discussed above, the current assessment of the gas pathway considers the degradation of carbon-14 labelled organic wastes. Nirex has also carried out work to identify additional sources of C-14 in UK waste and to include the potential release of C-14 containing gases from such wastes in a simplified model of gas generation.

Sources of C-14 in UK wastes

This section summarises a review of the sources of C-14 in the UK inventory and the potential for C-14 to be released as a gas from such wastes [4].

Irradiated steel

Carbon-14 could exist in irradiated steel in the form of elemental carbon or as a range of carbides. It may be the case that elemental carbon remains in its solid form following corrosion of the steel, however carbides of iron, chromium and nickel are hydrolysed with water to produce hydrocarbons.

Irradiated Zircaloy

Carbon-14 in Zircaloy may be in the form of stable zirconium carbide. Leach tests on Zircaloy fuel cladding have shown the production of carbon-14 in organic form in low concentrations in the liquid phase.

Irradiated Magnox

Carbon-14 may be present as magnesium carbide in Magnox metal. Corrosion of Magnox metal in a repository would result on exposure of the carbide, leading to formation of acetylene or ethylene.

Irradiated uranium metal

Irradiated uranium metal in wastes might contain carbon-14 as uranium carbide. Uranium carbides could hydrolyse to produce methane, acetylene or other hydrocarbons.

Irradiated aluminium

Carbon-14 in aluminium may exist in the form of aluminium carbide, decomposing in water to produce methane.

Irradiated graphite

Limited data suggests that carbon-14 could be released at low rates from graphite by reaction of the carbon with dissolved oxygen in water. This would lead to production of carbon dioxide, which, given the alkaline near field conditions, would dissolve or precipitate as calcium carbonate.

Barium carbonate

It is considered unlikely that C-14 containing gases could be generated from barium carbonate wastes.

Organic wastes

The UK inventory contains a mixed waste stream of simple organic molecules labelled with C-14. Microbial degradation of these wastes would lead to gas production. Under aerobic conditions carbon dioxide would form. Under anaerobic conditions a mixture of carbon dioxide and methane would be generated, depending on, for example, the presence of sulphate and nitrate in the waste.

An illustration of the relative contributions of these sources to the total carbon-14 inventory is provided in Table 2, on the basis of the 1998 UK National Radioactive Waste inventory (although the 2001 inventory is now available, it has not yet been analysed in this way). Carbon-14 from organic wastes is shown to be a relatively minor contributor to total carbon-14 in the inventory considered.

Tab. 2: Wastes Containing Carbon-l4 in each Waste Type Category: 1998 Inventory

Waste Type Category	Activity (TBq)	Fraction Activity in 1998 Inventory
Stainless Steels	1.2E+03	26.56%
Mild Steels	5.0E+02	11.21%
Zircaloy	2.1E+01	0.47%
Magnox	2.9E+01	0.66%
Uranium	4.7E+00	0.11%
Other Metals	7.7E+00	0.18%
Solid Graphite	1.8E+03	39.60%
Graphite Dust	4.5E+01	1.02%
Barium Carbonate	2.1E+02	4.65%
Organics	6.7E+02	15.12%
Contaminated Resins	2.9E+00	0.07%
Concrete	1.6E+01	0.36%
Ferric Hydroxide Floc	4.3E-01	0.01%

New "Simplified Model Of Gas Generation" (SMOGG)

Nirex has recently developed (with Serco Assurance) a model to calculate rates of gas generation from radioactive waste, known as a "simplified model of gas generation" (SMOGG) [5], for use throughout Nirex in its assessments of gas generation during the transport, operational, and post-closure phases of radioactive waste disposal. The model is simplified relative to the GAMMON model of gas generation that has been used to date by Nirex in its post-closure and some other assessments, and is intended as complementary to GAMMON, rather than as its direct replacement. The need for a simpler model basically derives from the difficulty in validating GAMMON, and providing justified values for the large number of input parameters required for the rather complex model present in GAMMON of gas production by microbial degradation of organic materials.

SMOGG includes a capability to model the release of C-14 containing gases from corrosion of irradiated metal, from microbial degradation of organic wastes and by leaching of activated graphite.

Gas generation from wastes depends on environmental conditions, in particular availability of water and oxygen and the temperature. Coupling between gas generation processes has been

included in an approximate way to provide an adequate treatment of the consumption of water and oxygen, without introducing unnecessary complexity to the model. In the model it is assumed that there is a specified amount of water initially present in the package, which is available for consumption by gas generation processes. Once this water is consumed, further water is made available at a constant rate to represent diffusion of water into the container or resaturation. Once the container is resaturated, water is considered to be unlimited. During transport and storage, it is assumed that the environment within waste containers is aerobic. Post-closure, the oxygen remaining in the vaults at closure has to be consumed before conditions become anaerobic.

Release of C-14 from corrosion of activated metals

It is assumed that C-14 in irradiated metals is present as metal carbides and that it is converted to methane when the carbide comes into contact with water. The user can specify the amount of C-14 present in the waste metal and the initial distribution. Corrosion models allow for aerobic and anaerobic corrosion reactions, with acute and chronic corrosion rates. The user can specify the initial corrosion rate and specify temperature dependence. The C-14 release rate is calculated from the corrosion rate, assuming that the waste metal is initially in the form of a sphere with specified radius (for calculation of the surface area).

Microbial degradation of organic wastes

Two classes of substrate are considered for the microbially mediated production of gases: cellulose and small, soluble organic molecules. The cellulose is initially hydrolysed to small organic molecules, which are then degraded to produce carbon dioxide and methane in the same way as any such molecules that are initially present. Methane is only produced under anaerobic conditions and in the absence of nitrate and sulphate, so these conditions are accounted for in the model.

It is considered that the cellulose might be hydrolysed by two distinct routes: first, under neutral or acid conditions via glucose-like monomers; secondly, under alkaline conditions via small molecules, of which ISA is the main component. Both routes are included in the model. The model also includes degradation of organic wastes by radiolysis.

C-14 is incorporated into the gases produced in proportion to the ratio of C-14 to C-12 in the pool of small organic molecules from which gas is being generated.

Release of C-14 from leaching of irradiated graphite

A simple empirical model calculates the release of C-14 from graphite based on the mass of graphite present, the initial activity of C-14 in the graphite and a rate constant for the initial release rate. It is assumed that the C-14 is released as carbon dioxide.

Carbonation

The user can specify what fraction of the carbon dioxide produced reacts with grout or cement backfill. C-14 that forms carbon dioxide and reacts with cement by carbonation is assumed not to reach the biosphere.

Comparison of SMOGG and GAMMON Active Gas Generation

The assessment of the gas pathway in the 2003 update of the Nirex suite of generic documents used the gas generation model GAMMON. In GAMMON the model of microbial degradation of cellulose includes explicit representation of microbial reactions and the outputs have been difficult to validate against experimental data. In a comparison exercise, SMOGG has been parameterised with the data used in the 2003 generic documents update for the unshielded intermediate level waste inventory, and the results are shown in Figure 1. Only carbon-14 from microbial degradation is considered here; no contribution to the carbon-14 source term arises from e.g. irradiated metals or graphite; also, carbon dioxide is assumed to react with repository cementitious materials, and will not be released to the biosphere. The details of repository operation and closure underlying Figure 1 are provided in Table 3; see [6] for further information:

Tab. 3: Repository Operation and Closure Timing and Conditions

Stage	Year	Temp (°C)	Water availability	Oxygen availability
Emplacement	2040 - 2090	35	Pore space in containers initially water filled	Aerobic
Care and maintenance	2090 - 2140	35	Continue	Aerobic
Backfilling and closure	2140-2150	80 for 5 years 50 for 5 years	Continue	Aerobic
Post-closure	2150 -	50 for 100 years 35 subsequently	Resaturates all pore space	Oxygen present at closure is consumed

In Figure 1, the comparison of both tritium generation rates and radon-222 generation rates are satisfactory. Comparison of SMOGG and GAMMON generation rates for carbon-14 bearing gases are markedly different, reflecting differing approaches taken in the codes to the production of such gases. It is not possible to say at this stage, in the absence of appropriate experimental data, which calculations are the most 'realistic'. For information, the legend actually identifies all the active gas considered in SMOGG; those indicated by a dashed line are not considered in calculation underpinning Figure 1.

Summary

There are a number of potential sources of C-14 in the UK radioactive waste inventory, which could be released as carbon-14 bearing gases. In addition to carbon-14 from microbial degradation processes, which is currently considered in Nirex assessment studies, a review indicates that carbon-14 that is present in irradiated metals in the form of metal carbides may be converted (on dissolution of the metal) into acetylene or methane gas. It is also possible that carbon-14 bearing gas may be produced from graphite, although initial work indicates that this is unlikely.

A new "simplified" model of gas generation has been developed (SMOGG). The model includes a capability to model the release of C-14 bearing gases from corrosion of irradiated metal, from microbial degradation of organic wastes and by leaching of activated graphite. The new model has been compared with the alternative gas generation model, GAMMON, which is currently used in Nirex assessment studies, for carbon-14 gas generated by microbial degradation. Further work will be undertaken using SMOGG, to assess the potential consequences of carbon-14 gas generation from metal carbides and graphite.

Reference models have so far assumed that any C-14 released as carbon dioxide will be consumed by reaction with the in-drum cementitious grout and/or the cement backfill. As this carbonation reaction is slow, the efficiency of carbon dioxide removal needs to be demonstrated.

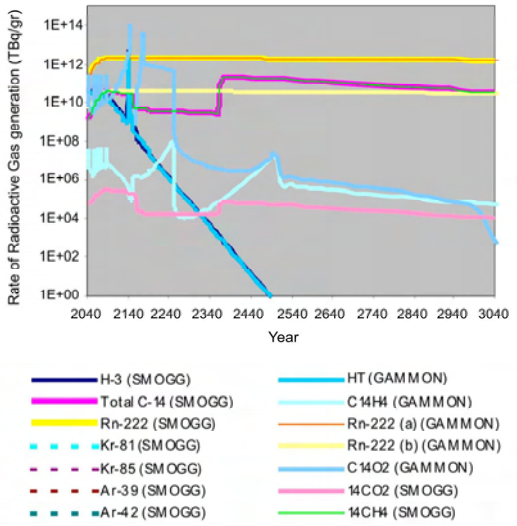

Fig. 1: Comparison of SMOGG and GAMMON Active Gas Generation Rates, on Basis of Unshielded Intermediate Level Waste Inventory from 2003

References

Nirex reports can be obtained by contacting: info@nirex.co.uk.

---

[1] Nirex, Generic Repository Studies, The Nirex Phased Disposal Concept, Nirex Report N/074, 2003.

[2] Nirex, Generic Repository Studies, Generic Post-Closure Performance Assessment, Nirex Report N/080, 2003.

[3] Nirex, Nirex 97: An Assessment of the Post-closure Performance of a Deep Waste Repository at Sellafield, Nirex Science Report S/97/012, 1997.

[4] T.W. Hicks, MB Crawford & DG Bennett, Carbon-14 in Radioactive Wastes and Mechanisms for its Release from a Repository as Gas, Galson Sciences Ltd Report 0142-1, 2003.

[5] WR Rodwell, Specification of a Simplified Model of Gas Generation from Radioactive Wastes, Serco Assurance Report SERCO/ERRA-0452 Version 3, 2003.

[6] A.R. Hoch & W.R. Rodwell, *Gas Generation Calculations for Generic Documents Update, 2003*, Serco Assurance Report SA/ENV-0514 Version 2, 2003.